A Comprehensive Study on CO_2-CH_4 Gas Separation Using γ-Alumina Membrane and Parameters Affecting Permeability and Separation Behavior

FATIN MUNIRAH BINTI AHMAD

CHEMICAL ENGINEERING

UNIVERSITI TEKNOLOGI PETRONAS

SEPTEMBER 2012

CERTIFICATION OF APPROVAL

A Comprehensive Study on CO_2-CH_4 Gas Separation Using γ-Alumina Membrane and Parameters Affecting Permeability and Separation Behavior

by

Fatin Munirah Binti Ahmad

A project dissertation submitted to the

Chemical Engineering Programme

Universiti Teknologi PETRONAS

in partial fulfilment of the requirement for the

BACHELOR OF ENGINEERING (Hons)

(CHEMICAL ENGINEERING)

Approved by,

_____

(Dr. Norhayati Binti Mellon)

UNIVERSITI TEKNOLOGI PETRONAS

TRONOH, PERAK

September 2012

CERTIFICATION OF ORIGINALITY

This is to certify that I am responsible for the work submitted in this project, that the original work is my own except as specified in the references and acknowledgements, and that the original work contained herein have not been undertaken or done by unspecified sources or persons.

_____

FATIN MUNIRAH BINTI AHMAD

ABSTRACT

Membrane separation has emerged as one of the most vital and practical useful modern separation techniques. Membrane-based gas separation is an important unit operation for the separation of many gas mixtures in oil and petrochemical industries such as acid gases removal like CO_2 and H_2S from natural gas and organic vapors removal from air. This report comprises the basic introduction of research area which includes background on membrane usage, types of membrane for intended separation and problems associated with this separation. The objective of this study is to develop mathematical model for CO_2-CH_4 separation using γ-alumina membrane and analyse parameters affecting permeability and separation behavior. Meanwhile, the scope of work is divided into development of permeability models for various transport mechanisms, development of membrane balance, simulation work for numerous parameters testing and analysis of permeability and separation performance. The methodology is divided into two algorithms for permeability and separation perfomance respectively.

Generally, the permeability is expected to increase with higher pore size, higher pressure and lower temperature. As for selectivity, smaller pore and lower temperature is better. Other than that, lower stage cut results in lower CH_4 loss, higher CO_2 retained and higher CO_2 removed. Meanwhile, higher feed CO_2 will increase the amount of CO_2 removed and CO_2 retained.

ACKNOWLEDGEMENTS

First and foremost, I would like to express my appreciation and praise to Allah for His guidance and blessing throughout my entire project work. I would also like to sincerely thank UTP for giving me this opportunity to involve in this particular research area.

I would like to express my utmost appreciation for my supervisor, Dr. Norhayati Mellon for guiding me with valuable insights throughout the whole project.

Besides that, thousands of gratitude goes to all the examiners, lecturers and colleagues involved for their constructive criticisms and cooperation.

Finally, an honourable mention goes to my family and friends for their understandings and also support on completing this project.

TABLE OF CONTENTS

LIST OF FIGURES

LIST OF TABLES

CHAPTER 1

INTRODUCTION

1.1 Background of Study

Membrane technology is one of the emerging technologies with a broad spectrum of application. Dutta (2007) defines membrane as a thin barrier placed between two phases or mediums which allow one or more constituents to selectively pass from one medium to another while retaining the rest. The separation occurs with the presence of an appropriate driving force such as concentration, temperature, pressure or electrical gradients.

1.1 .1 The Use of Membrane

Membrane processes are designed to carry out physicochemical separations (Judd, 2003). Membrane separation has emerged as one of the most important, practical and useful modern separation techniques in chemical process industries and many other fields. Membrane-based gas separation is an important unit operation for the separation of many gas mixtures in oil and petrochemical industries. For examples, moisture removal, air separation into high-purity nitrogen and oxygen-rich air, acid gases removal such as CO_2 and H_2S from natural gas and organic vapors removal from air (Madaeni, 2010). According to Carreon (2012), this separation is of great interest from the environmental and energy perspectives as effectively capturing carbon dioxide has a positive impact to the environment and reducing undesirable impurities content as from energy point of view. Normally, natural gas which is obtained directly from gas well composes 4 to 50% of CO_2. CO_2 is the number one greenhouse gases (GHG) and an acid gas which is highly corrosive and rapidly destroys pipeline and equipment. It also decreases the heating value of a natural gas stream and wastes pipeline capacity. Typical pipeline quality states that the CO_2 composition in the treated gas stream must not exceed 2% (Safari, 2008).

Figure 1.1 illustrates the typical gas separation process using membrane where the feed mixture is separated into individual permeate and retentate stream. Permeate stream

consists of the part of the feed mixture that pass through the membrane while retentate is where the species does not pass through the barrier and is retained. In this CO_2-CH_4 separation, theoretically, the permeate stream consists of CO_2 and other impurities and the retentate side will retain CH_4.

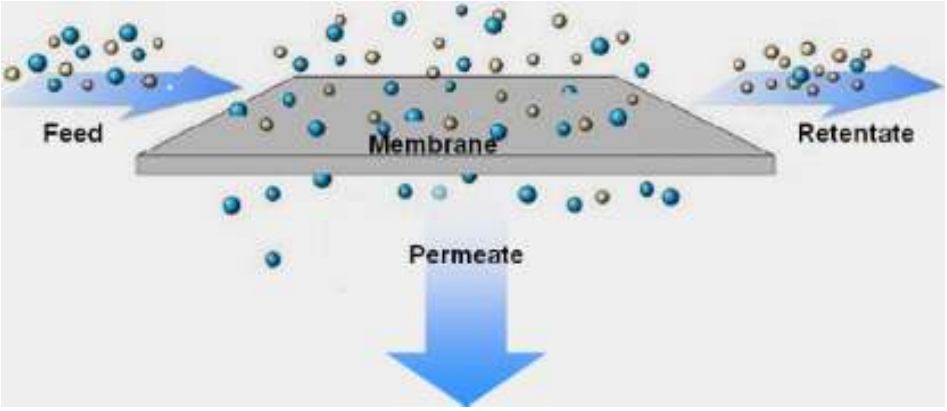

Figure 1.1: Membrane Gas Separation Process (Schmeling, 2010).

1.1.2 Types of Membrane for CO_2 Separation

CO_2 is an infamous acid gas contains in natural gas. A well can reach as high as 95% CO_2 content due to enhanced oil recovery (EOR) application where high-pressured CO_2 is pumped into depleting oil reserves to drive residual oils to existing oil wells. Not only that, the acid gas content is also varied by its geographical location whereby Poland, Germany, Pakistan and New Zealand are among the highest while Malaysia only contain 7% (Spillman, 1989).

One of the major applications of membrane technology includes gas separation using membrane. As cited by Okada and Nakagawa, since 1950s, numerous researches emerged to develop new materials for practical gas separation. Mostly, membranes used for gas separations are organic or polymeric such as cellulose acetate, polyimidies and polysulphones (Freeman and Pinnau, 1999). However, inorganic membrane such as ceramic are quite widely used in variety of applications, from nanofiltration and water purification to gas separation due to their structural robustness, thermal stability, chemical resistance and reliability. One of the disadvantages of using organic membrane

is, at high pressure, the plasticization effect of CO_2 will affect the separation performance. Meanwhile, compared to α-alumina, γ-alumina is a very fine-grained alumina that occurs in a cubic spinal structure but converts readily to the alpha phase in sintering temperatures. However, gamma powder has a very high specific surface area of about 100 square meters per gram. In this particular separation, γ-alumina is an excellent ceramic membrane which exhibits high chemical resistance and long stability in water also with an operating temperature up to 1000^{o}C (Synkera, 2010). Mukhtar (2010) reaffirms that the use of γ-alumina has several advantages which it possess the characteristics of structural robustness, thermal stability, chemical resistance and reliability, efficient, and low cost. Thorough preparation steps for mesoporous alumina are discussed in by the Group of Inorganic Material Sciences Protocol from the Ohio States University (Yu, 2005).

1.1.3 Problems Associated in CO_2 Membrane Separation

Even though there are other competitions towards membrane usage in gas separation such as absorption, cryogenic distillation, and pressure-swing adsorption (PSA); which is high cost and complex, the uses of membranes offer few advantages. As stated by Spillman and Sherwin, membranes require low capital investment, ease of installation and operation, absence of rotating part, process flexibility, low weight and space requirement, and least environmental impact. Not only that, the possibilities of no additional utilities such as compressor is needed if the feed readily contained high-pressured gas.

Nevertheless, if compared to absorption process, for membranes to meet pipeline quality for CO_2 is economically challenging. Not only is that, hydrocarbon losses very low in absorption. Hydrocarbon recovery is also a factor especially in a single stage membrane system, where hydrocarbon loss is only economically feasible from 2% to 10% (Safari, 2008). However, single stage system is recommended for low flow application and multi stage is more applicable at higher flow rates to reduce the loss of hydrocarbon. In order to make CO_2 gas separation using membrane more appealing, higher permeability and separation performance are the two crucial parameters to be achieved.

1.2 Problem Statement

Fundamental membrane study is crucial to develop further understanding in this maturing technology. Membrane gas separation is deemed to be more attractive and simple than existing technologies. Compared to existing basic membrane models, many are lacking in identifying the overall separation performance as a function of various affecting parameters and hydrocarbon losses. Other than that, the proposed model will take into account all contributing permeability models which are the transport mechanisms occurring in common membrane. Most models also had high degree of complexity and difficult in computing. This study is using the modeling & simulation approach as empirical and experimental studies for membrane can be time consuming and expensive. Therefore, in order to develop further understanding in gas separation using membrane process, mathematical models development and simulation is expected to be very beneficial. The permeation and separation behavior mechanism is deemed as a function of various process influences. Plus, mathematical models can efficiently generate behavior trends without acquiring much cost. Figure 1.2 summarized the difference for experimental and simulation approaches.

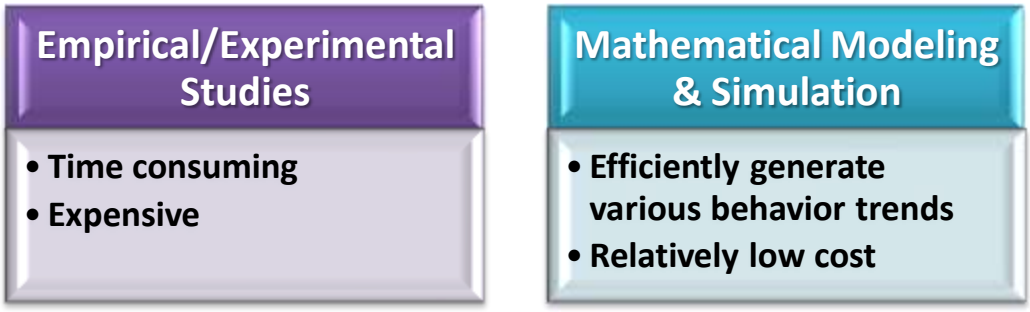

Figure 1.2: Comparison between Experimental and Simulation Approaches.

1.3 Objectives and Scope of Study

The objective of this project is based on the SMART (Specific, Measurable, Achievable, Relevant, Time-Limited) approach. The main objective expected to be achieved by the end of this study is:

- To develop mathematical model for CO_2-CH_4 separation using γ-alumina membrane and analyse parameters affecting permeability and separation behavior.

The scopes of the study of the said project are as follow:

- Develop permeability models for various transport mechanisms.
- Develop mathematical equation of membrane balance using complete mixing model.
- Develop simulation model as a function of pore size, pressure, temperature, stage cut and feed CO_2 composition.
- Permeability and separation performance analysis.

This research will contribute the permeability and separation factor data as a function of various process parameters with analysis on its separation performance summarizing the quality trends of removal, retained and loss composition.

CHAPTER 2

LITERATURE REVIEW

In this chapter, screening of published research journals and articles are done to integrate pertinent and important information which supports the relevance of this project. Therefore, as we go along, there are numerous researches discussed in this chapter which are related to the evolution and development of membrane technology, either experimental or simulation-based.

As explained by Kazama (2004), an ideal membrane material is when the membrane layer is perfectly rejecting the unwanted species. This research is owned by Research Institute of Innovative Technology for the Earth (RITE) which was established in July 1990, as one of the cores research organization with the objective to develop innovative environmental technologies and CO_2 sinks expansion. The table below summarized the comparison of polymeric and ceramic membrane according to selectivity required for process gas. Based on the data in table below, it is safe to conclude that ceramic membrane, which is used in this project, performs better as opposed to polymeric. Yet, hundreds of research continues to grow in developing the 100% selectivity with at least 95% of the species will result in the desired streams for the new concept membrane. Moisture may also cause blockage to the gas permeation process.

Table 2.1: Polymeric vs. Ceramic Membrane (Feed Gas Composition 6:4).

Membrane Type	CO_2/H_2 Selectivity	After Separation (H_2:CO_2)	
		H_2 Side	CO_2 Side
Polymeric	0.3	4:1	5.5:4.5
Ceramic	0.1	9:1	3.8:7.2

Quoted from Chenar (2005), 'the polarization effect increases at higher stage cuts'. This causes the reduction in CO_2 removal with increasing stage cut. The study by Chenar is using polyimide hollow fiber membranes. The result can be clearly seen in the Figure 2.1 below.

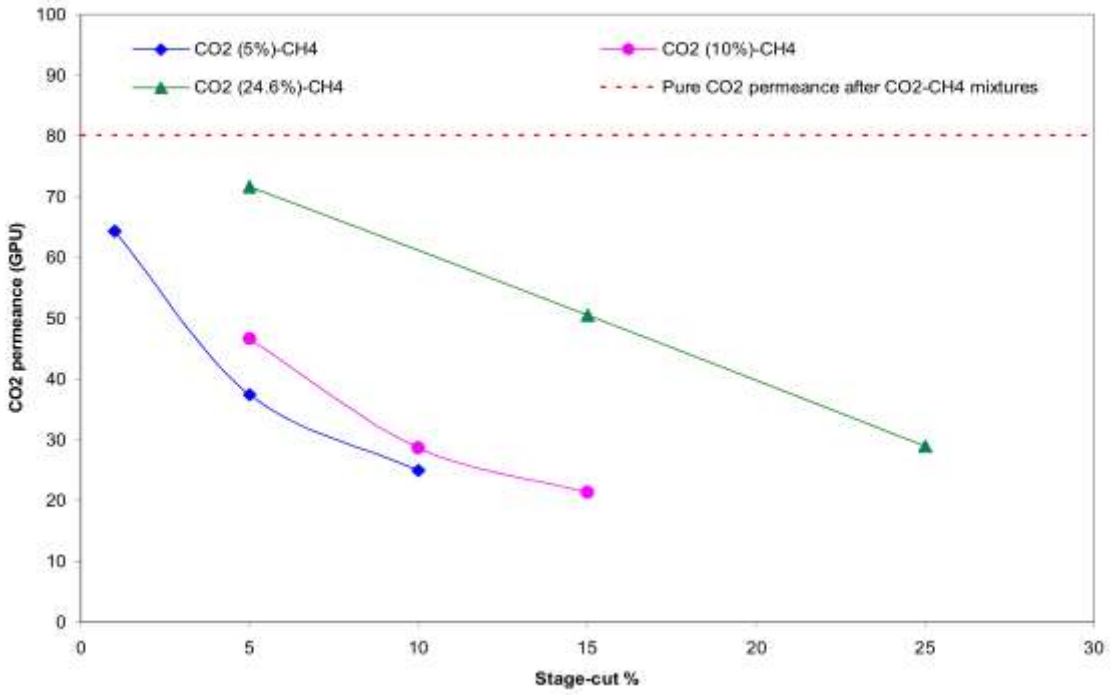

Figure 2.1: Permeability vs. Stage Cut for Various Feed Concentrations (Source: Chenar)

According to Himeno (2007), CO_2 separation and recovery are of great interest from the global warming and energy conservation point of views. Amine adsorption is among the technology used for this desired adsorption. Nevertheless, amine plants are very complex and consume a lot of money and maintenance. Therefore, membrane separation is more energy-efficient. In this paper, an inorganic membrane of zeolite is chosen as organic membranes shows a low tolerability to various temperature ranges. Zeolites are inorganic crystalline structures with uniform molecular dimensions, greater thermal, chemical, mechanical, and high-pressure stability. The proposed plant schematic diagram and zeolite structure can be seen as in Figure 2.2 and 2.3.

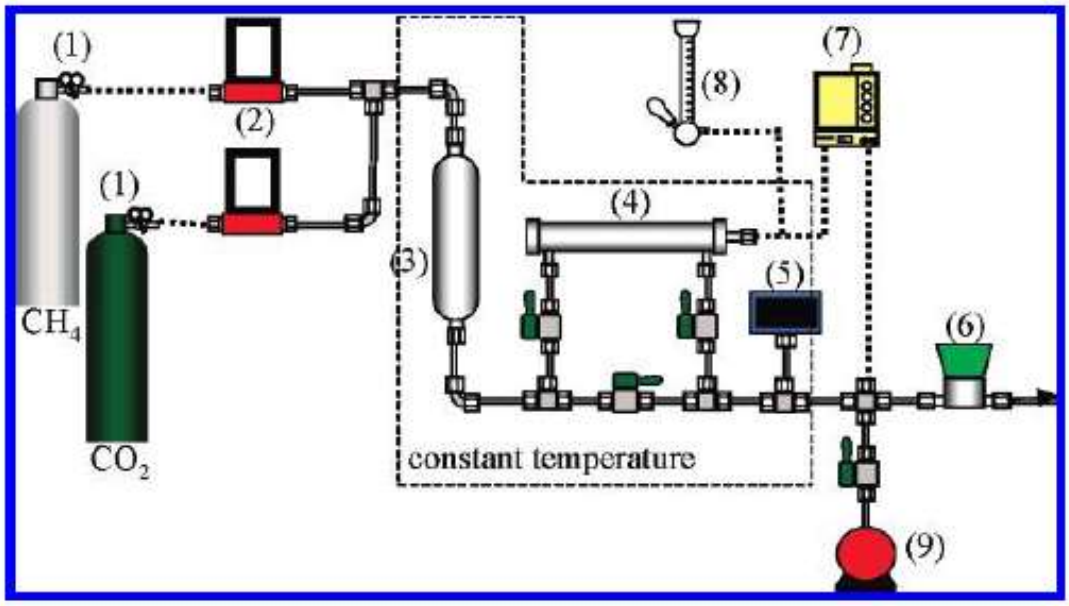

Figure 2.2: Schematic Diagram of Separation Experimental Apparatus (1) feed gas cylinder; (2) mass flow controller; (3) gas mixing vessel; (4) zeolite membrane cell; (5) pressure transducer; (6) back-pressure regulator; (7) TCD gas chromatograph; (8) soap film flow meter; and (9) rotary vacuum pump (Source: Himeno).

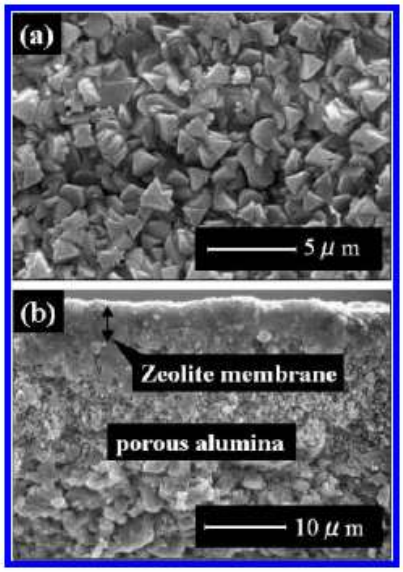

Figure 2.3: Microstructure of Zeolite Membrane by Electron Microscopy (a) Surface and (b) Cross Section (Source: Himeno).

Norhayati (2009), in her research has suggested to develop the simplest and accurate model that is able to depict the performance of membrane for natural gas dehydration by using cross flow model on a hollow fibre module. Saturated vapour from air stream and natural gas is removed using membrane. Nevertheless, the methane losses and condensation of gas on the membrane wall are among the common complexity arising. Mathemathical models are very helpful to simulate membrane performance, and finding the simplest model is the most anticipated of all. In her work which is also presented during the 7th International Conference on Membrane Science and Technology (MST), a relationship on methane losses at various stage cut is shown to be proportional.

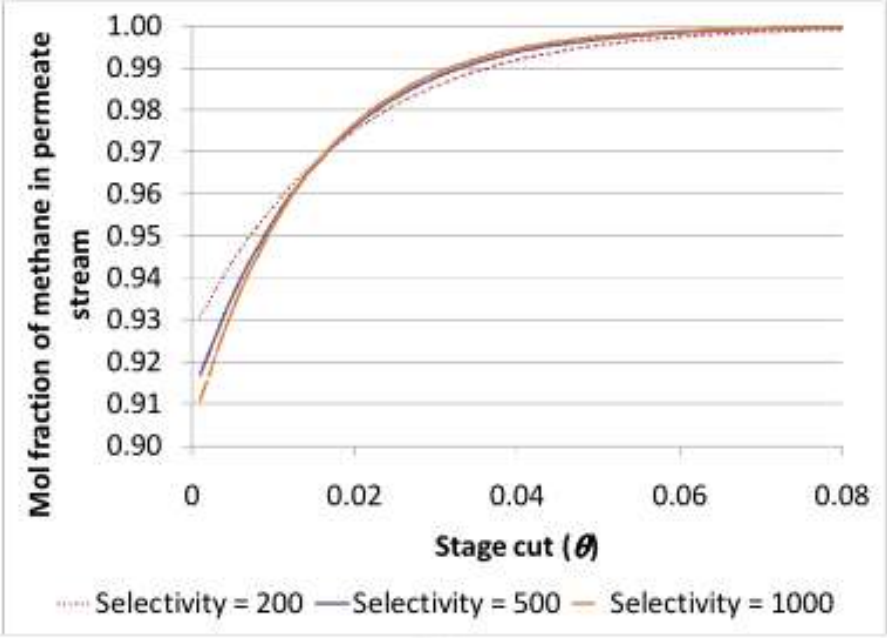

Figure 2.4: Variation in CH_4 Mol Fraction in Permeate (Source: Norhayati).

Boributh (2009) published a journal which justify the effect of temperature and feed composition to its flux (permeability) using a hollow fiber membrane contactor. Membrane wetting is related to temperature increment due to blockage and condensation effect. On the other hand, higher feed CO_2 composition is said to increase the permeability.

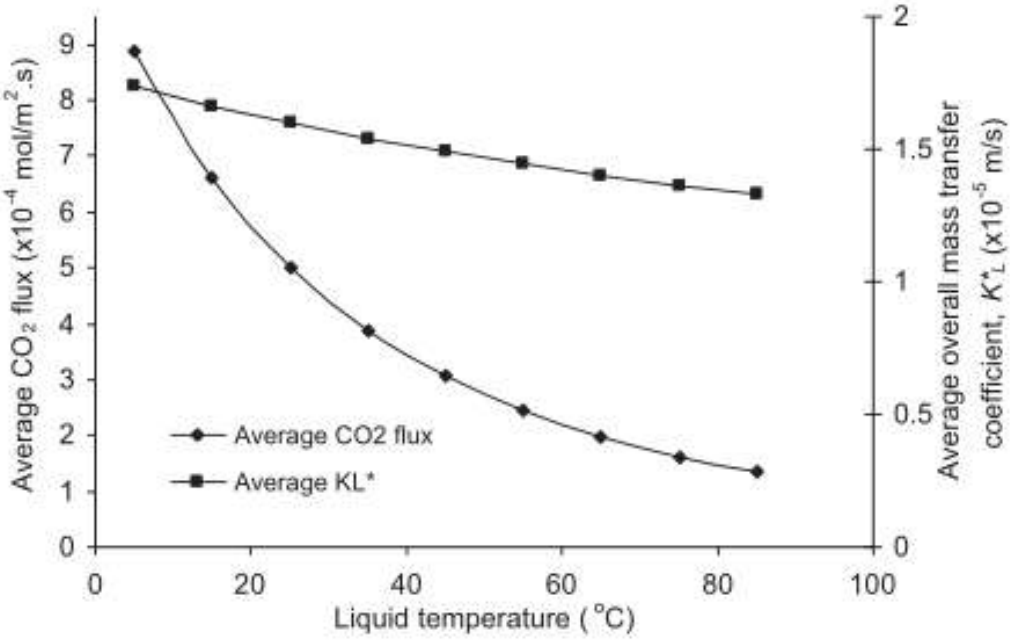

Figure 2.5: Permeability vs. Temperature (Source: Boributh).

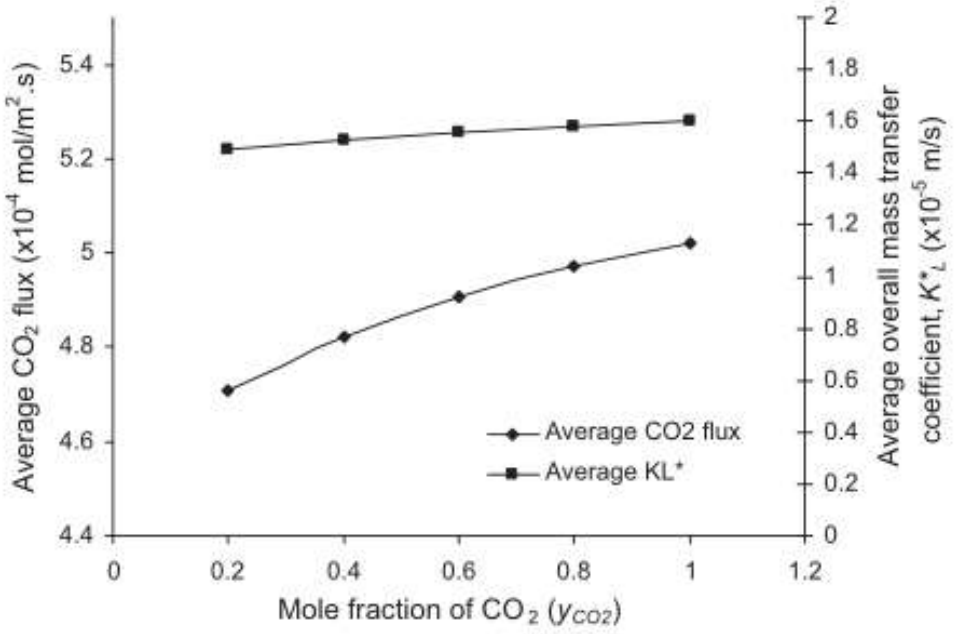

Figure 2.6: Permeability vs. Fed Gas Composition (Source: Boributh).

Science Direct is one of the most infamous search engines for educational journals. In this case, a research done by Safari, an optimization for CO_2 removal from natural gases using simple glassy polymers membrane models (cellulose acetate) as a function or temperature and pressure. The journal was accredited under the International Journal of Greenhouse Gas Control by the year of 2009. Optimization is crucial to decrease the hydrocarbon loses by using multiple-stages separation.

This research is done at a base case condition where several assumptions as below are applied:

- ✓ Ideal gas law is applied for all for process streams.
- ✓ Pressure drops in the membrane high-pressure side is neglected.
- ✓ Membrane module temperature drops is neglected.
- ✓ Permeability and selectivity affected by mixed-gas permeation is neglected.
- ✓ CO_2 plasticization effect is negligible.
- ✓ Spiral-wound elements cost = 70 $\$/m^2$.
- ✓ Methane loss cost = 0.5 $\$/m^3$.
- ✓ Membrane useful life = 3 years.
- ✓ Overall cost is the sum of two costs (membrane cost + methane lost cots in useful life).

From the examination perform on the chosen membrane, the result has shown to adhere to the theory and the experimental data. The theory results are calculated using the equation following the form of partial-immobilization model. With the coefficient determined as 0.99, the result for permeability is depicted in Figure 2.7 based on various temperature and pressure. In general, the increment in temperature is proportional to permeability while pressure is inversely proportional to permeability. The deviation rate witnessed is higher at lower pressure.

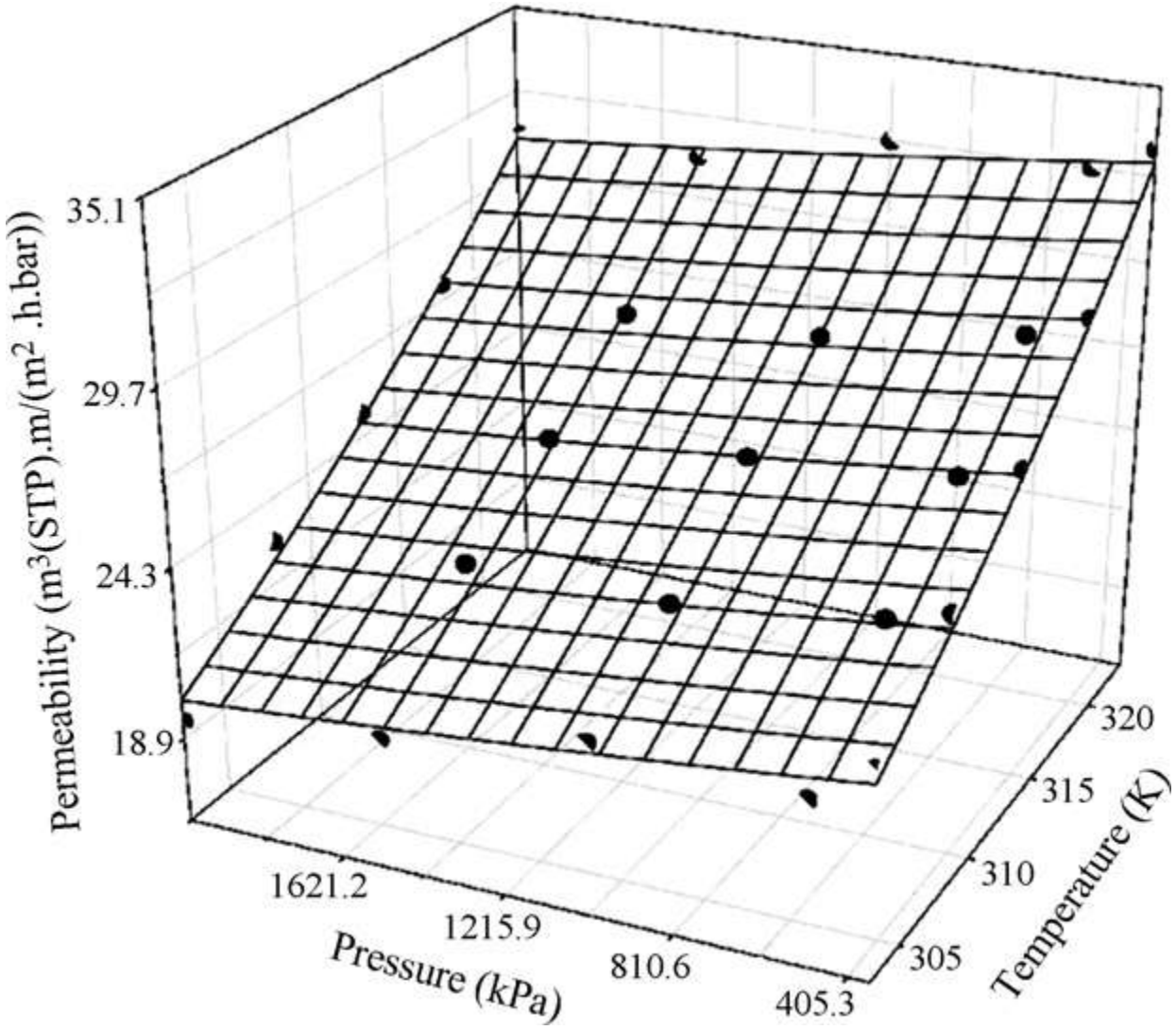

Figure 2.7: CH_4 Experimental Predicted Permeability Data (Source: Safari).

As for selectivity for CO_2/CH_4 separation behavior, as shown in Figure 2.8, both temperature and pressure increase causing the selectivity to decrease with solubility is subjected to be constant towards various pressure ranges to abide by Langmuir condition. Nevertheless, the temperature is described to be more significant in causing change in selectivity data. However, the pressure increment is affecting the diffusivities to increase as well, which is also omitted in this case.

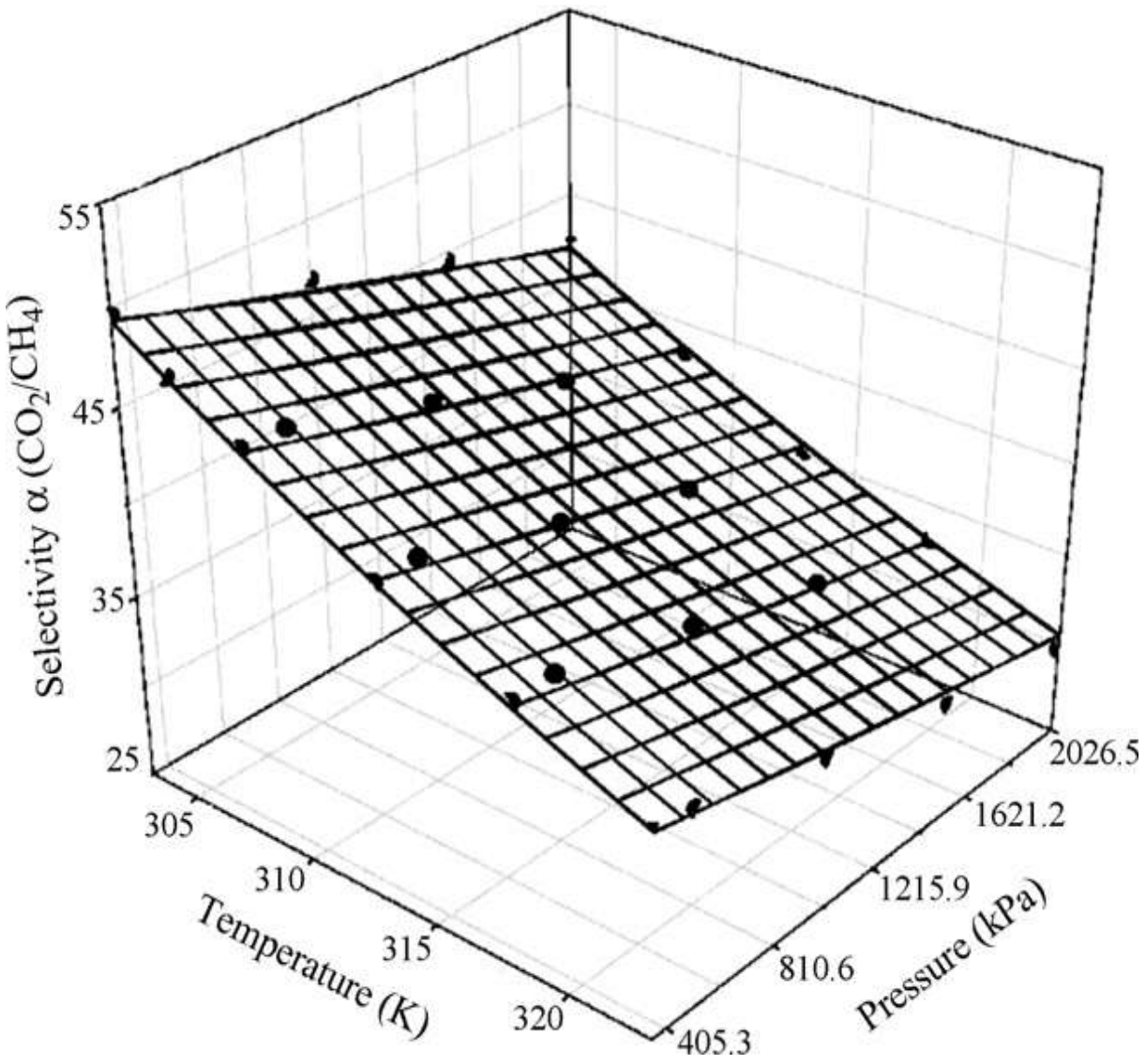

Figure 2.8: CO_2/CH_4 Experimental Selectivity Data (Source: Safari).

For the two-stage membrane process, which is performed to achieved methane loss not more than 2%, two fundamental design parameters are considered which are total area (first and second stage) and recycle flow rate.

As a whole, the permeate pressure is deemed to be highly affecting optimization process and cost for various permeate pressures. Meanwhile, certain minimum total stage area need to be achieved to reduce the methane loss, as well as the CO_2 contained in feed load which if bulkier, will induce higher methane loss.

Lau (2010), in his thesis published by World Academy of Science has shown the methane recovery for different feed CO_2 composition with various operation systems including recycle and multiple stages. The research is based on a cross flow model membrane. Figure 2.9 shows that methane recovery is higher with lower feed concentration of CO_2.

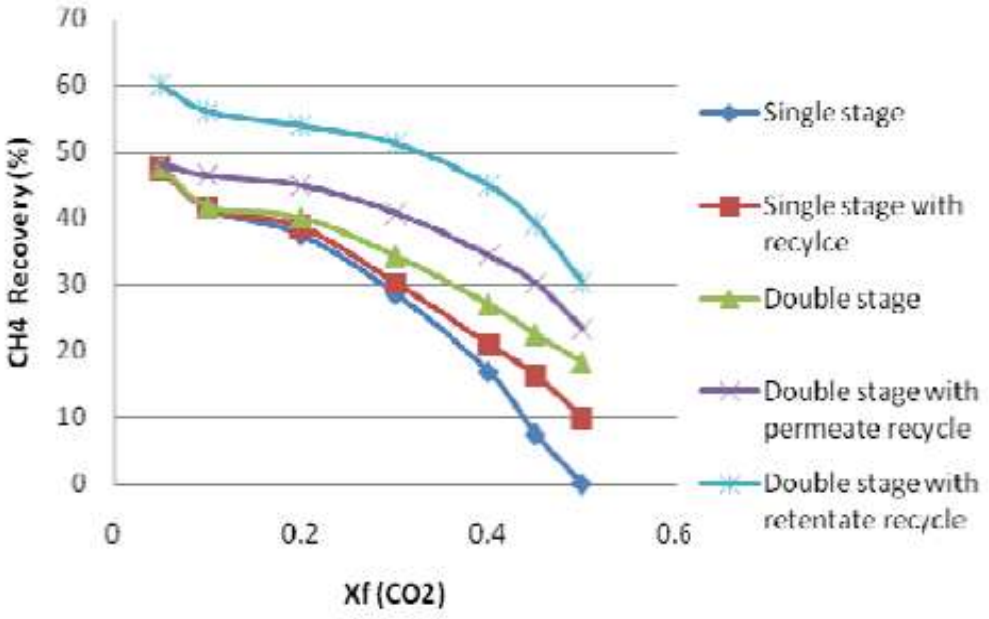

Figure 2.9: Methane Recovery vs. Feed Composition (Source: Lau).

Mukhtar performed another mathematical study to compare predictive models to determine the CO_2 permeability in Matrimid-Carbon Molecular Sieve (CMS) Mixed Matrix Membrane. The research was published by Journal of Applied Sciences in 2010. This membrane is a combination of organic and inorganic membranes to produce an impeccable membrane as conventional membranes posed several limitations for the use of membrane in gas separation.

Abedini (2010), in his study on membrane application in gas separation, has reaffirmed the advantageous on membrane technology mainly that use inorganic membranes. The journal has also discussed on various transport mechanisms in which surface diffusion is said to be the best yet.

Carreon's work in her research published by The Royal Society of Chemistry on January 2012 supports that CO_2-CH_4 separation is of great interest. The journal demonstrates the synthesis of reproducible and unremitting AIPO-18 membrane for CO_2-CH_4 separation with high permeability and separation selectivity. AIPO-18 membrane is synthesized with aluminium tri-sec-butoxide and aluminium isopropoxide with an in situ crystallization which is supported on a stainless steel. This intended separation is deemed to be the most economically feasible in terms of energy and environmental.

Figure 2.10 below provides a graphical description on the AIPO-18 membrane with small pores which causes the membrane to favour diffusion.

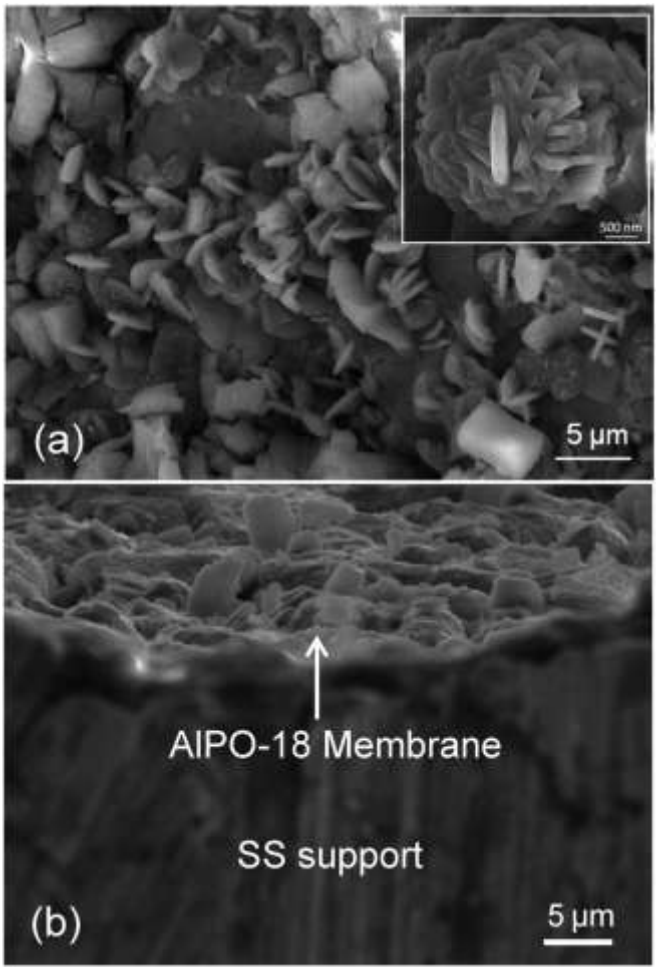

Figure 2.10: Microstructure of AIPO-Membrane (Source: Carreon).

As of 2012, Indian Journal of Chemical Technology revised a mathematical study of CO_2-CH_4 in a hollow fibre module by Madaeni. The CO_2-CH_4 separation study applied a counter current hollow fibre module as the feed flows into the shell. The mathematical method is used to estimate the separation behavior at various conditions. The research also highlighted that membrane technology presents lower capital and utility costs. Other than that, the simulation study offers better understanding thus avoiding time-consuming empirical studies.

In a nutshell, there are numerous research mostly modeling than experimental, are done on this maturing membrane technology. Therefore, it is suffice to state that membrane research is one of the most relevant fringes to be chosen as focus project area as countless number of industries and processes depending on membrane technology development. Therefore, in further chapters, fundamental concepts, theories and mathematical models related to membrane gas separation will be explained thoroughly and methodology framework shall be clearly outlined in order to perform permeability and separation performance analysis.

CHAPTER 3

THEORY

3.1 Flux and Permeability Concepts

'Flux' is one of the important concepts for membrane transport where flux is expressed by the unit of [$mol.m^{-2}.s^{-1}.Pa^{-1}$]. As opposed to flux which is normalized per unit pressure, 'permeation' or 'permeability' is normalised per unit of thickness [$mol.m.m^{-2}.s^{-1}.Pa^{-1}$].

3.2 Pore Types

As for porous materials, there are numbers of parameters that influence transport properties such as pore size and shape, and porosity. There are three main categories for pore types which are macropore, mesopore and micropore (descending in size). Figure 3.1 below also depicted the different types of pores existed in porous membrane (Burggraaf, 1996).

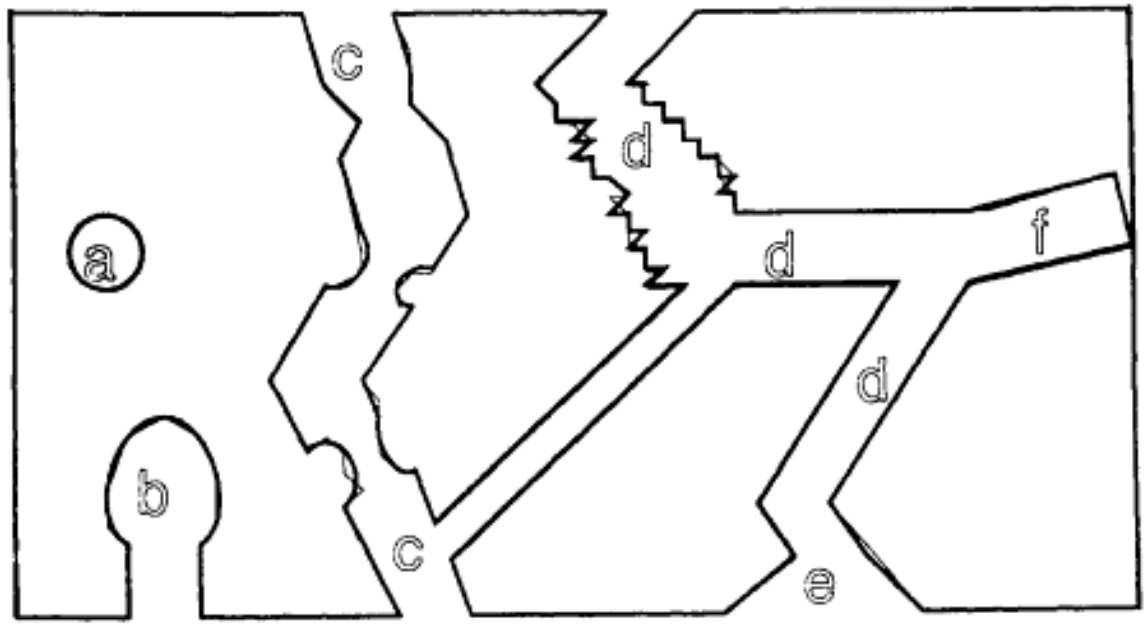

Figure 3.1: Schematic Picture of Pore Types in a Porous Membrane. (a) Isolated Pore; (b),(f) Dead End Pore; (c),(d) Tortuous and/or Rough Pores; (e) Conical Pore.

3.3 Transport Mechanisms

There is several transport mechanism in porous membranes such as capillary condensation, Knudsen diffusion, and many more (Basile, 2011). The different transport mechanisms in porous membranes are presented below:

1. Poiseuille (Viscous) Mechanism

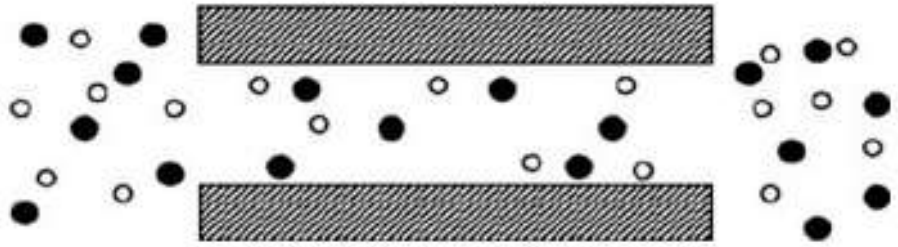

Figure 3.2: Poiseuille (Viscous) Mechanism.

This mechanism occurs when the average pore diameter is bigger than the average free path of fluid molecules. In this case, no separation takes place.

2. Knudsen Mechanism

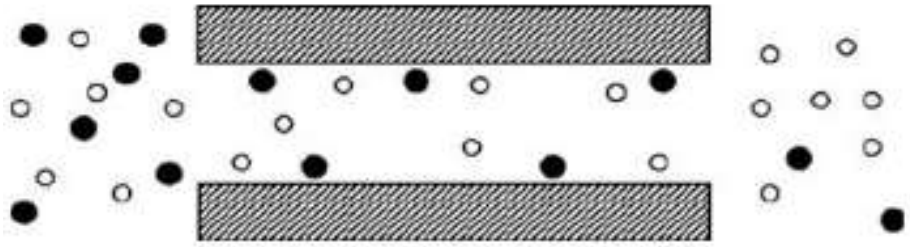

Figure 3.3: Knudsen Mechanism.

When the average pore diameter is similar to the average free path of fluid molecules, Knudsen mechanism takes place.

3. Surface Diffusion

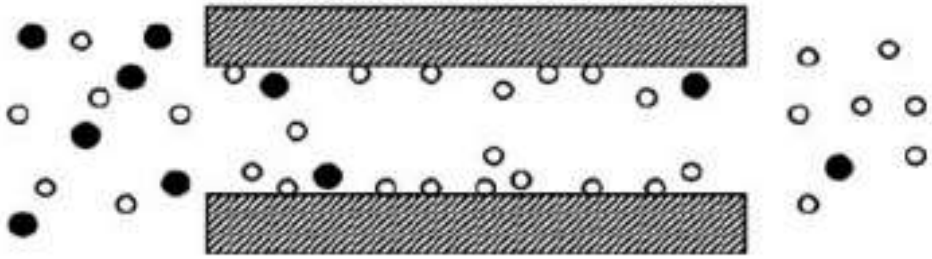

Figure 3.4: Surface Diffusion.

This mechanism is achieved when one of the permeating molecules is adsorbed on the pore wall. This type of mechanism can reduce the effective pore dimensions obstructing the transfer of different molecular species.

4. Capillary Condensation

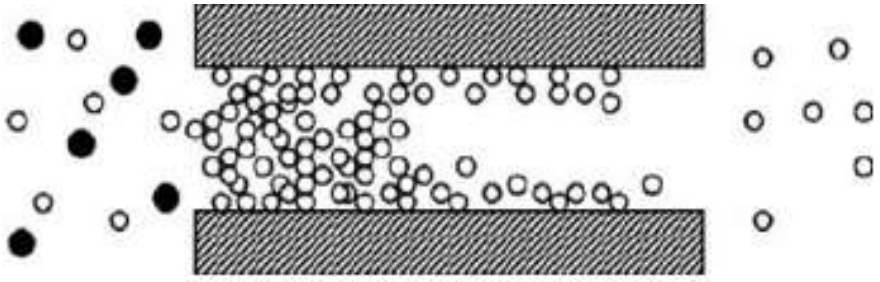

Figure 3.5: Capillary Condensation.

This type of mechanism takes place when one of the components condenses within the pores due to capillary forces. Generally, the capillary condensation favours the transfer of relatively large molecules.

5. Multi-layer Diffusion

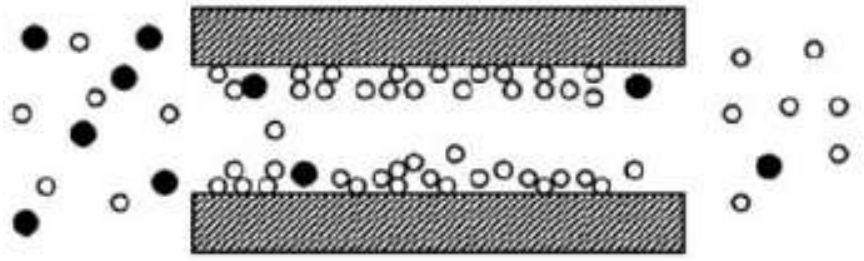

Figure 3.6: Multi-layer Diffusion.

When the molecule–surface interactions are strong multi-layer diffusion occurs. This mechanism is like to an intermediate flow regime between surface diffusion and capillary condensation.

6. Molecular Sieving

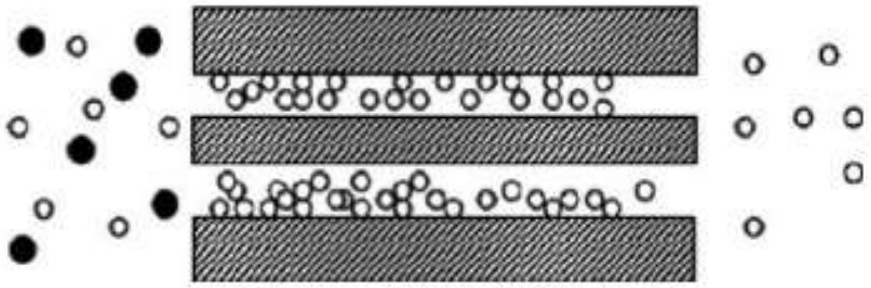

Figure 3.7: Molecular Sieving.

This takes place when pore diameters are very small, allowing the permeation of only the smaller molecules.

In summary of transport types, Poiseuille flow is non-selective while Knudsen diffusion poses large effect on the permeability. Surface diffusion occurs at small pore regions with highest selectivity and capillary condensation causes plasticizing effect of CO_2.

3.4 Gas Permeability Model

As stated in part 3.1, permeability is an important parameter in membrane transport. Commonly, the gas permeability measurement is done on pure gas species. In general, permeability of a polymer for a gas mixture increases with decreasing size and increasing solubility or condensability of the gas. The relative permeability of a gas is given below in order of decreasing gas permeability as:

$$\mathbf{H_2 > He > H_2S > CO_2 > O_2 > Ar > CO > CH_4 > N_2}$$

There are several other empirical models which are developed for gas permeability prediction for various transport mechanisms.

The permeability of component-i is a product of two terms:

$$P_i = K_i \cdot D_i \tag{3.1}$$

where K_i is the sorption (or partition) coefficient and D_i is the permeate diffusion coefficient.

In gas separation, the membrane selectivity is used to compare the separating capacity of a membrane for two or more species. The membrane selectivity, α (also known as the permselectivity) for one component (A) over another component (B) is given by the ratio of their permeabilities:

$$\alpha_{AB} = \frac{P_A}{P_B} \tag{3.2}$$

Replacing for P_A and P_B, and re-arrange, we have:

$$\alpha_{AB} = \frac{K_A}{K_B} \cdot \frac{D_A}{D_B} \tag{3.3}$$

The ratio D_A/D_B is the ratio of the diffusion coefficients of the two gases and can be viewed as the mobility selectivity, reflecting the different sizes of the two molecules. The ratio K_A/K_B is the ratio of the sorption coefficients of the two gases and can be viewed as the sorption or solubility selectivity, reflecting the relative condensabilities of the two gases.

3.5 Flow Models

Geankoplis (2003) suggested several important of flow pattern types are as in Figure 3.8 and 3.9. A detailed process flow diagram is shown for complete mixing. When a separator element is operated at a low recovery such as where the permeate flow rate is a small fraction of the entering feed rate, there is a minimal change in composition. Then the results derived using the complete-mixing model provides reasonable estimates of permeate purity. In the case of cross-flow, the longitudinal velocity of the high-pressure or reject stream is large enough that this gas stream is in plug flow and flows parallel to the membrane. On the low-pressure side the permeate stream is almost pulled into vacuum, so that the flow is essentially perpendicular to the membrane. These two cases were derived by Weller and Steine. Flow patterns are important in determining the composition with respect to location inside a model. Despite for not taking non-isothermal effect, the idealized complete mixing model will be explored as it is more practical at this stage.

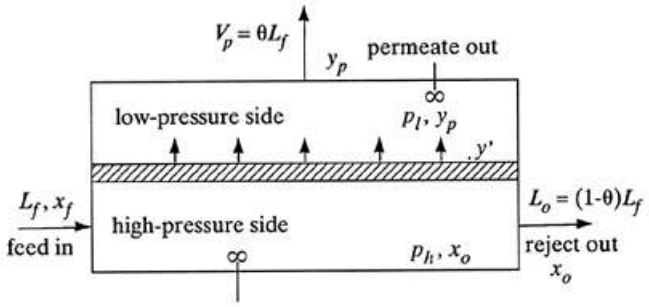

Figure 3.8: Complete Mixing Model.

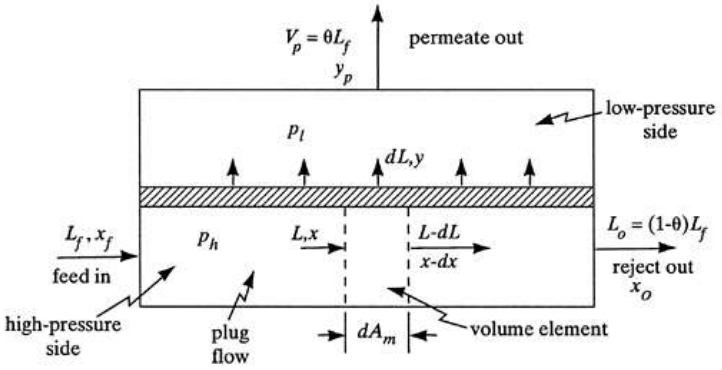

Figure 3.9: Cross-flow Model.

3.6 Viscous Diffusion

Permeability is a function of pore size. Each of the gas viscosity, μ_i, can be calculated by using Bird (1960) empirical correlation which varies depending on the temperature and directly affecting the permeability.

$$\mu_i = 2.6693 \times 10^{-5} \frac{\sqrt{T \cdot M_i}}{\sigma^2 \Omega_\mu} \quad (3.4)$$

Where: T = Temperature (K); M_i = Molecular Mass (g/mol); σ = Collision Diameter (Å);

Ω_μ = Product of Collision Integral and Reduced Temperature.

3.7 Gas (Knudsen) Diffusion

Knudsen diffusion, $D_{k,i}$, is imperatively dominates as the gas molecules and pore walls collision frequency increases. The Knudsen diffusion is valid when the pore size, r_p, is bigger than gas molecules, r_g.

$$D_{k,i} = \frac{2(r_p - r_{g,i})}{3} \sqrt{\frac{8RT}{\pi M_i}} \quad (3.5)$$

Where: R = 8.314 J/K.mol.

3.8 Surface Diffusion

Surface diffusion, D_s, takes place when the gas temperature is crucial for the pore walls adsorption.

$$D_s = 1.6 \times 10^{-2} e^{\left[-0.45 \frac{(-\Delta H_{ads})}{mRT}\right]} \quad (3.6)$$

Where: m = 2 for conductive sorbent and 1 for non-conductive sorbent.

3.9 Gas Permeability with Transport Mechanisms

The permeability of gas as a result of viscous diffusion, $P_{vis,i}$, as given below.

$$P_{vis,i} = \varepsilon \cdot \frac{(r_p)^2\left(\frac{P+1.2}{2}\right)}{8\tau\mu_i zRT} \tag{3.7}$$

Where: ε = porosity; τ = tortousity.

The permeability of gas as a result of Knudsen diffusion, $P_{k,i}$, as given below.

$$P_{k,i} = \frac{\varepsilon\left(\frac{1}{\frac{1}{D_i}+\frac{1}{D_{k,i}}}\right)}{z\tau RPT} \tag{3.8}$$

The permeability of gas as a result of surface diffusion, $P_{s,i}$, as given below.

$$P_{s.i} = \frac{2\varepsilon^2 t_m(1-\varepsilon)D_{s,i}\rho_m f_i}{z\tau^2 RPT r_{p,i}} \tag{3.9}$$

Where: t_m= membrane thickness; ρ_m= membrane density; f_i= loading factor.

3.10 Separation Factor

Ideal separation factor, α_i, is influenced by the molecular weights of components.

$$\alpha^* = \sqrt{\frac{M_B}{M_A}} \tag{3.10}$$

Where: $M_B > M_A$.

However, the actual separation factor, α, gives the effect of back diffusion (Burggraaf, 1996).

$$\alpha = 1 + \frac{(1-P_r)(\alpha^*-1)}{1+P_r(1-y)(a^*-1)} \tag{3.11}$$

3.11 Complete Mixing Model

As explained in part 3.5, figure 3.8 depicts the complete mixing model. As proposed by Weller and Stein, the rejection composition, x_o, and permeate composition, y_p can be calculated as below.

Let A = CO_2 and B = CH_4 :

Overall material balance of figure 3.8:

$$q_f = q_o + q_p \tag{3.12}$$

The cut of permeate and feed flow, θ:

$$\theta = \frac{q_p}{q_f} \tag{3.13}$$

Rate of diffusion of component A = CO_2 and B = CH_4 :

$$\frac{q_A}{A_m} = \frac{q_p y_p}{A_m} = \left(\frac{P'_A}{t_m}\right)\left(p_h x_o - p_l y_p\right) \tag{3.14}$$

$$\frac{q_B}{A_m} = \frac{q_p(1-y_p)}{A_m} = \left(\frac{P'_B}{t_m}\right)\left[p_h(1-x_o) - p_l(1-y_p)\right] \tag{3.15}$$

Where: A_m = Area or membrane.

Divide equation 3.14 by 3.15,

$$\frac{y_p}{1-y_p} = \frac{a^*\left[x_o - (\frac{p_l}{p_h})y_p\right]}{(1-x_o)-\left(\frac{p_l}{p_h}\right)(1-y_p)} \tag{3.16}$$

Component A balance,

$$q_f x_f = q_o x_o + q_p y_p \tag{3.17}$$

Divide by q_f and replace with 3.13,

$$x_o = \frac{x_f - \theta y_p}{1-\theta} \tag{3.18}$$

CHAPTER 4

METHODOLOGY

4.1 Project Activities

Apart from understanding the basic fundamental of gas membrane separation, there will be two major project activities which are mathematical model development and model simulation as illustrated in Figure 4.1.

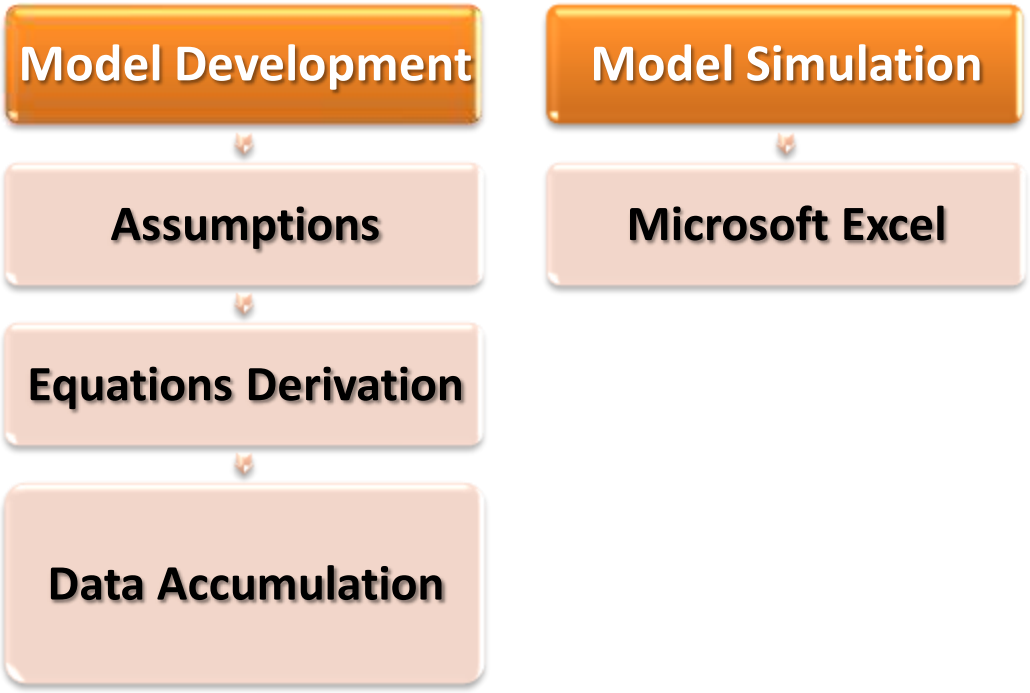

Figure 4.1: Main Project Activities

The two main activities are explained thoroughly as follows:

1. Model Development

i. In this step, several assumptions are made in order to develop a suggestive model such as the process is considered as isothermal, negligible pressure drop, no reaction occurs inside the membrane and system involves only two components (binary). The flow model selected is complete mixing model.

ii. There are numbers of basic equations selected and used in order to study the permeability and separation behavior of this binary mixture as discussed in Chapter 3.

iii. Membrane properties are another significant data to be obtained including pore size. Table 4.1 below illustrates the membrane properties of selected membrane for this study.

Table 4.1: γ-Alumina Properties (Keizer, 1988).

Pore size range, r_p (nm)	0.15 – 290.00
Membrane thickness, t_m (μm)	0.10
Porosity, ε	0.603
Tortousity, τ	1.658

2. Model Simulation

i. The model is simulated using the most user-friendly Microsoft Office Excel software version 2007 above. Excel is chose as it is highly integrated and sophisticated software that is capable to understand various mathematical functions and perform simple iteration. Other than that, Excel works in a spreadsheet form which can easily generate visual result.

4.2 Research Methodology

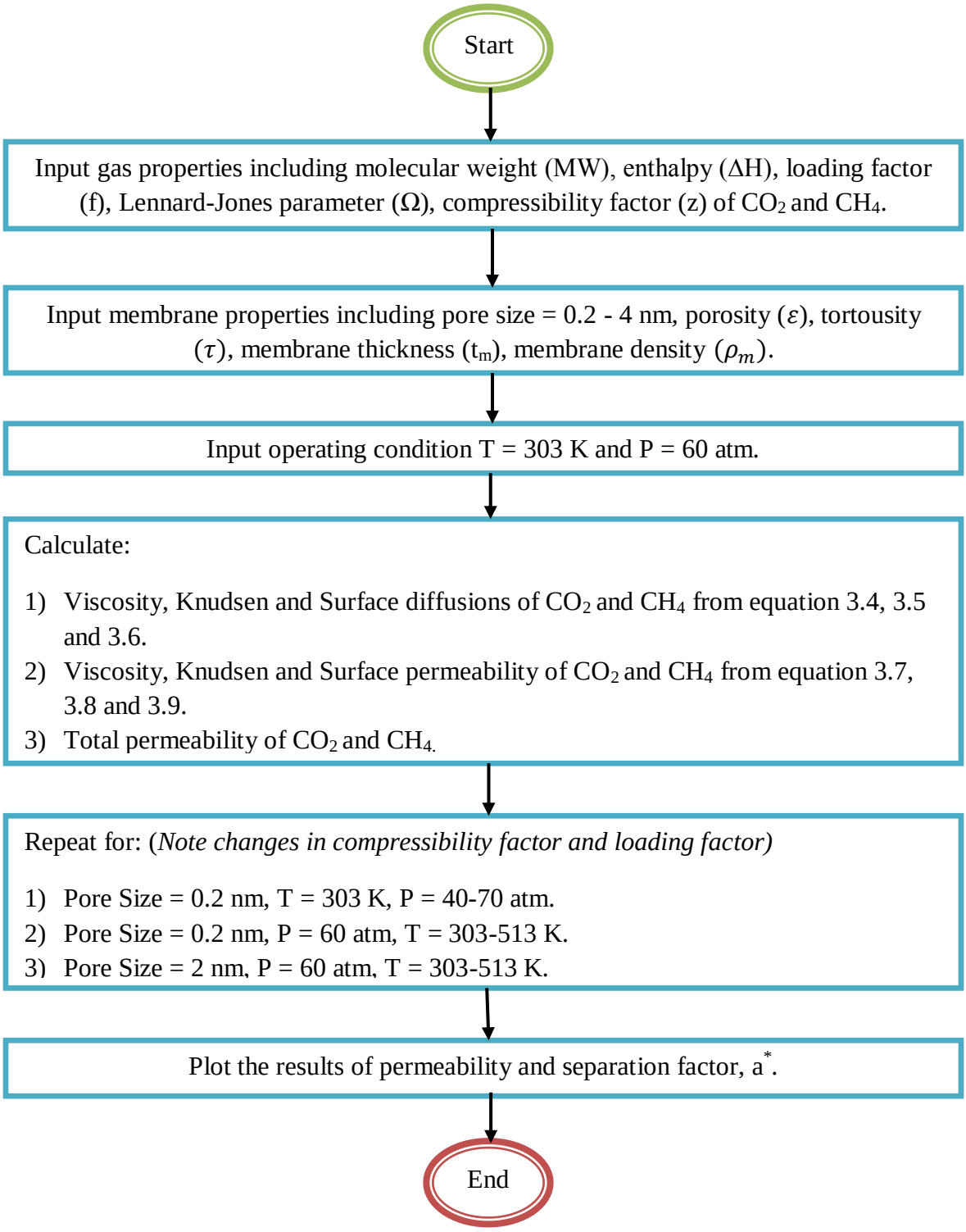

Figure 4.2: Algorithm for Permeability Model and Separation Factor.

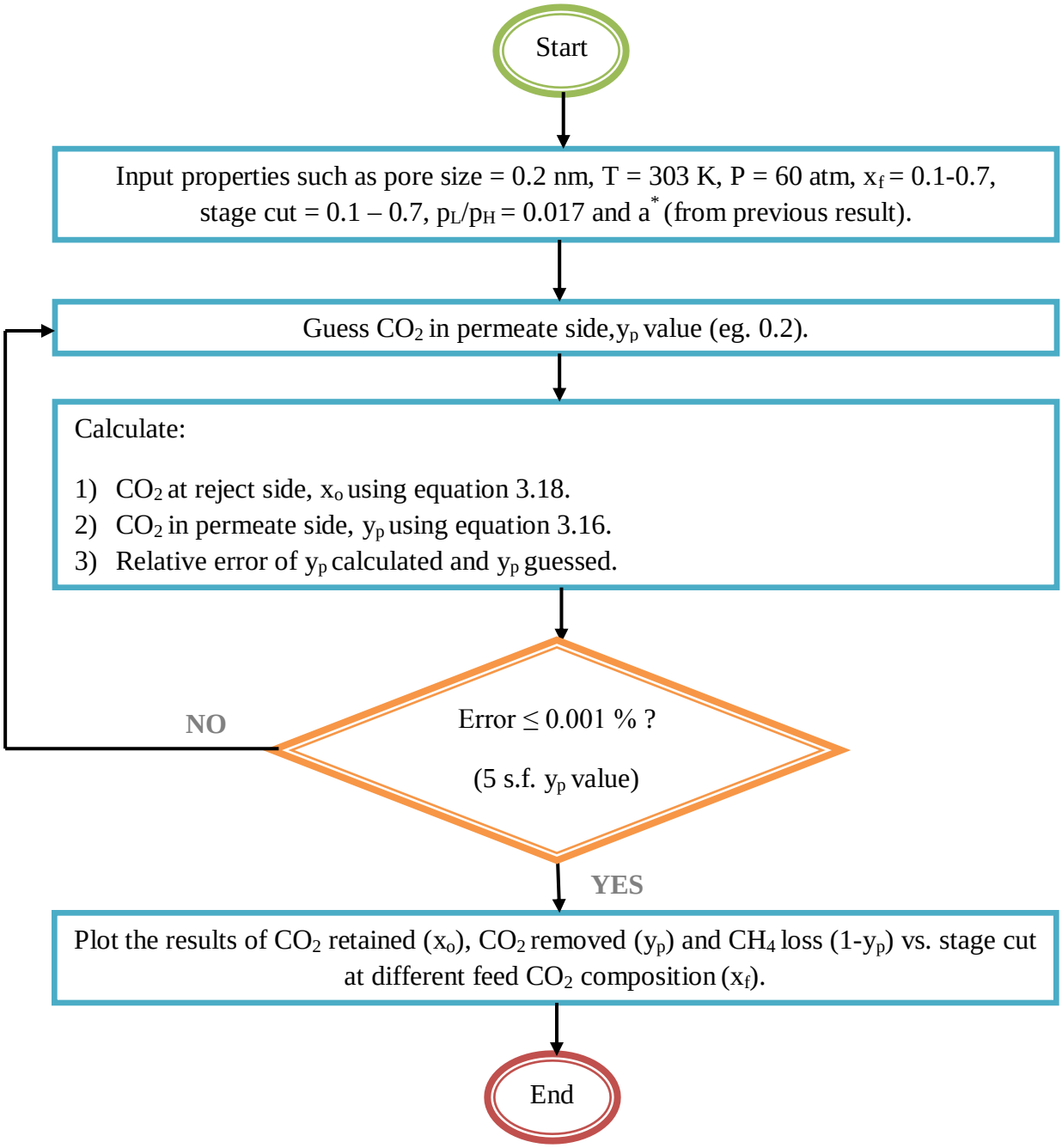

Figure 4.3: Algorithm for Separation Performance Analysis.

4.3 Tools

- Microsoft Office software version 2007 above such as Word, Excel and PowerPoint

4.4 Gantt Chart and Key Milestones

Table 4.2: Gantt Chart and Key Milestones.

Year	2012								2013
Semester	FYP I				FYP II				
Month	May	June	July	Aug	Sept	Oct	Nov	Dec	Jan
Activity									
Fundamentals of Gas Membrane Separation, Membrane Materials & Parameters Affecting									
Extended Proposal Submission		X 25th							
Proposal Defense			X 16th						
Model Development									
Interim Report				X 13th					
Model Simulation									
Progress Report							X 5th		
Analysis of Results									
Poster Presentation							X 26th		
Project Improvement									
Draft Report								X 3rd	
Soft Bound Dissertation								X 10th	
Technical Paper								X 10th	
Oral Presentation								X 21th	
Hard Bound Dissertation									X 11th

CHAPTER 5

RESULTS AND DISCUSSION

5.1 The Effect of Pore Size on Gas Permeability

One of the studies that will be carried out is to observe the trends of gas permeation in porous membrane in the pore size range of 0.2 nm to 2 nm. From the properties of γ-alumina membrane stated in Chapter 4, the pore size range is given as 0.15 nm to 290 nm. However, the selected pore size range selected in this study as suggested by Uhlhorn and Burggraaf which is in the normal range of gas separation. In addition, three transport mechanisms in gas permeation are studied individually as shown in Chapter 3.

Figure 5.1 and 5.2 illustrate the trend of CO_2 and CH_4 permeability as a function of pore size taking into consideration of various transport mechanisms affect on total permeability. As can be seen in Figure 5.1, at small pores, surface diffusion is more dominant in determining the total permeability. Knudsen and viscous diffusions are not significant as the smaller pore size is hindering the travel path. In equation 3.9, the pore size term is placed at the denominator of the surface permeability calculation. This means that when the pore size decreases, the acting surface permeability increases. The gas molecules is more likely to diffuse from bulk gas film to the smaller pore surface as higher concentration gradient takes place. If compared to Figure 5.2, CO_2 permeability is higher for pore size 1 nm and below where CH_4 permeation will dominate otherwise. The variation can also be explained as the surface diffusion (equation 3.6) shows that it is dependent on heat of adsorption of the gas specie. CO_2 has a lower heat of adsorption of -17116 J as compared to CH_4 , -21000 J (the negative terms represent that energy is released, exothermic, when adsorbate molecules are attracted to adsorbent surface). Higher heat of adsorption, in this case, CH_4, will result in higher surface diffusion and permeability. Surface diffusion is also deemed to be the most attractive and flexible preference for gas separation due to its selective diffusion (Abedini, 2012).

Nevertheless, at higher pore size, Knudsen is deemed to be more significant as the mean free path of gas molecule is higher. The effective mean free path can be deduced by the diameter of gas molecule and the pore diameter, where bigger difference will account for higher Knudsen diffusion and permeability. This justifies why the individual CO_2 Knudsen permeability is higher as CO_2 has a kinetic diameter of 0.33 nm while CH_4 is 0.388 nm. However, the overall comparison of permeability for both species shows that CO_2 permeability dominates at lower pore size. Since the

purpose of this gas separation is to remove CO_2, it is of our great interest to favour smaller pore size range preferably 0.2 nm as CO_2 removed is much higher. The result obtained can be relate to Abedini's (2010) work where the separation factor (permeability of desired specie) will continue to decrease until the pore size are small enough that the larger molecules, in this case CH_4, will be restricted at the membrane entrance.

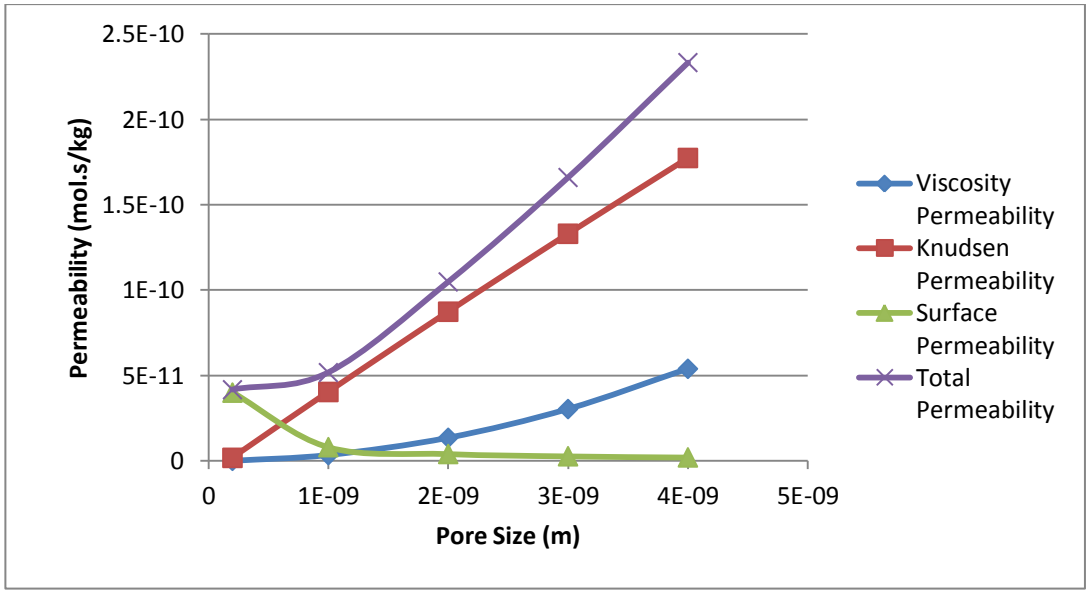

Figure 5.1:CO_2 Permeability at Various Pore Size (T = 303 K; P = 60 atm).

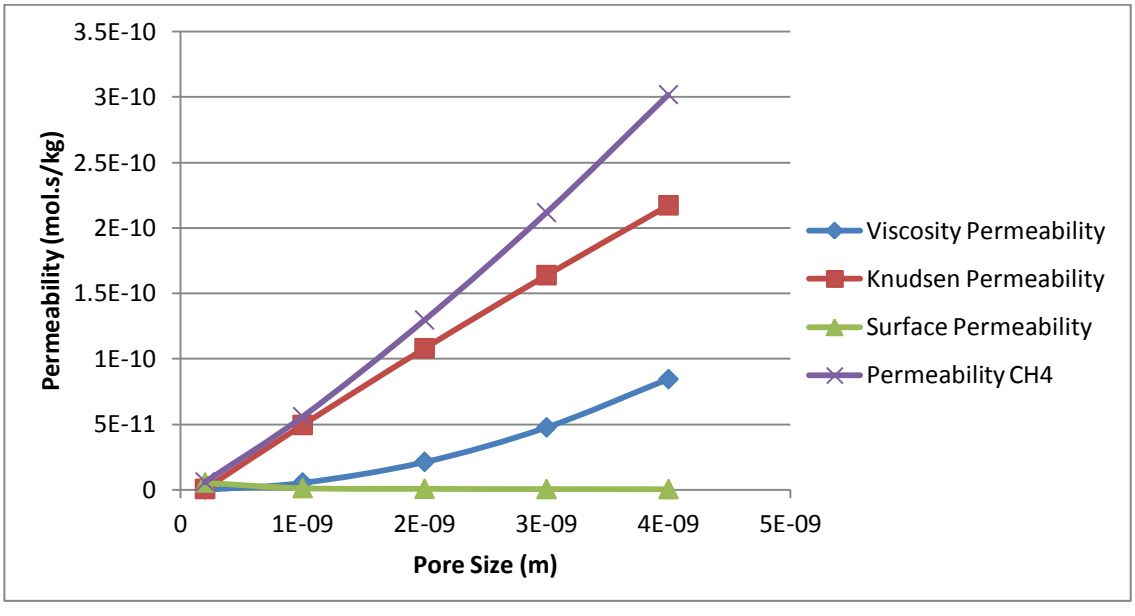

Figure 5.2: CH_4 Permeability at Various Pore Size (T = 303 K; P = 60 atm).

5.2 The Effect of Operating Pressure on Gas Permeability

The study of operating pressure affects on gas permeability is done by selecting operating pressure range of 40 to 70 atm. From all tested transport mechanisms, surface permeability is the most significant for CO_2 while viscous permeability determines the trend for CH_4 permeability variation. The effect of pressure is proved in equation 3.7 where the pressure term is in the numerator part where higher pressure will induce higher permeability. The result in Figure 5.3 is relevance with Chenar's (2005) study using polyimide membrane where increasing the pressure will increase the permeability of gas species as well. Here, it shows that driving force for pressure plays an important role in forcing the molecules to pass through membrane wall.

Nevertheless, the separation will become economically unattractive if the feed pressure of the gas is to be increased as operation dealing with high pressure is poses higher risks. Therefore, in this case, 60 atm is the most tolerable to be selected as the operating pressure because not only that extra higher pressure is costly and risky, it will reduce the selectivity of the gas separation as all species are force to pass through. The relationship of selectivity and pressure is confirmed by Bae (2008) where selectivity is significantly higher for lower pressure.

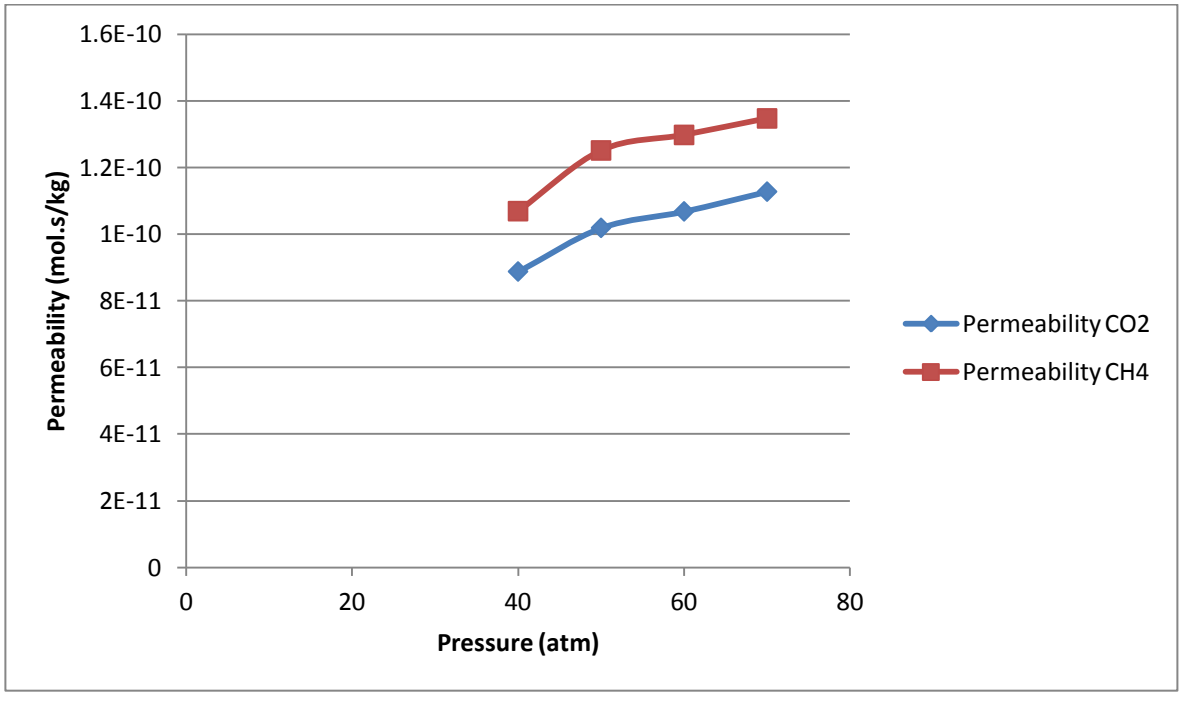

Figure 5.3: Comparison of Total Permeability for CO_2 and CH_4 at Various Operating Pressure (Pore Size = 0.2 nm, T = 303 K).

5.3 The Effect of Operating Temperature on Gas Permeability

For this part, the study of various operating temperature, 30 to 240 ^{o}C, is done at 60 atm operating pressure for two values of pore size, 0.2 and 2 nm. The tested values will help in illustrating the difference of small pore and big pore size especially for separation factor analysis later in part 5.4. As explained earlier that at small pore, 0.2 nm, surface permeability dominates both species overall permeability, while at big pore, 2 nm, Knudsen permeability is more momentous. The trends can be seen in Figure 5.4 and 5.5. However, a similar observation can be concluded for both pore sizes where the permeability decreases as temperature increases. This relationship can be clearly seen from equation 3.7, 3.8 and 3.9 where all individual permeability calculations involve temperature on the denominator side. The small increment of CH_4 permeability from 150 ^{o}C occurs in small pore due to the surface diffusion exponential term variation.

For bigger pore, this effect is hazed by the domination of Knudsen diffusion. The high temperature applied may also break the force (Van Der Waals) that holds the adsorbed molecules on the pore wall surface and decrease the molecular density. With that, it is expected that the permeability is to decrease when temperature increase. For that reason, the permeability is said to be best at 30 ^{o}C (or 303 K). The same relationship has also been established by Boributh (2009) where CO_2 flux is lower as temperature increases.

Most hydrocarbon streams also contain some portion of water that will cause the CO_2 to become soluble in water as temperature increases. The water could also vaporize and block at the membrane pores, thus, inhibiting other species to pass through (Boributh, 2009).

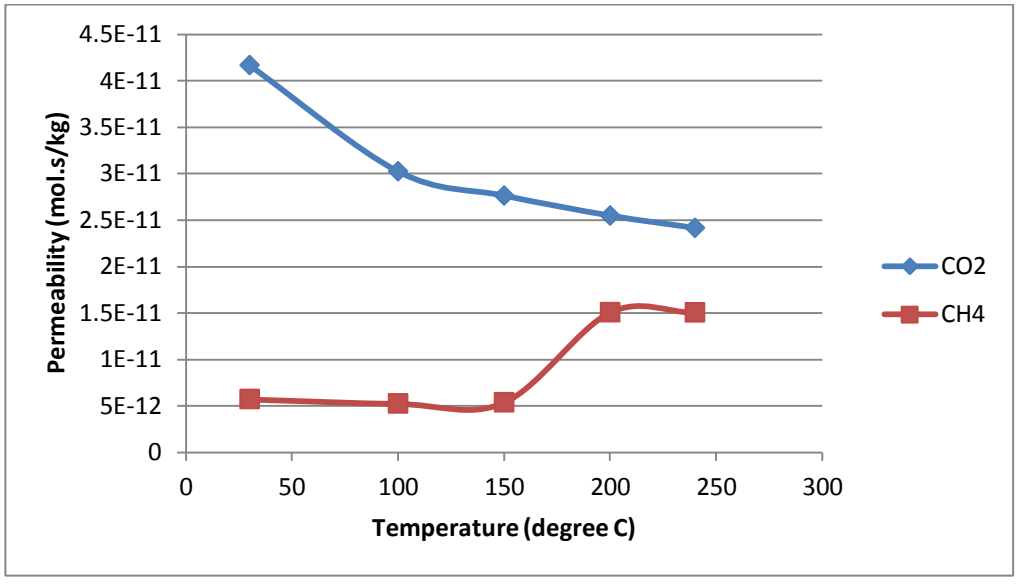

Figure 5.4: Comparison of Total Permeability for CO_2 and CH_4 at Various Operating Temperature (Pore Size = 0.2 nm, P = 60 atm).

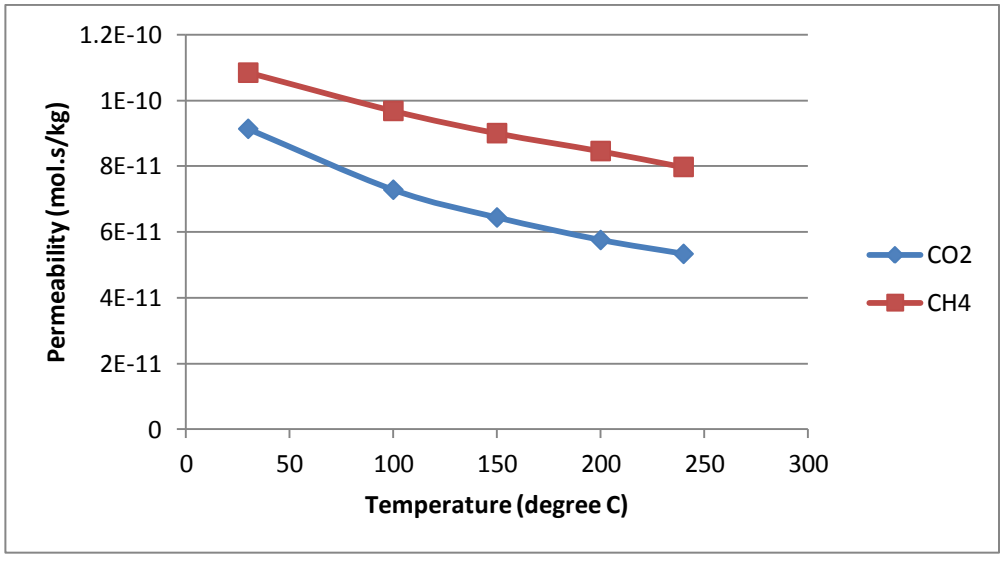

Figure 5.5: Comparison of Total Permeability for CO_2 and CH_4 at Various Operating Temperature (Pore Size = 2 nm, P = 60 atm).

5.4 The Effect of Operating Temperature on Separation Factor

Based on the result obtained in part 5.3, ideal separation factor is calculated using equation 3.2. In Figure 5.6, it is vividly observes that smaller pore at 303 K gives the highest separation performance. This is again caused as bigger pore will result in higher mean free path, thus, more molecules, will non-selectively pass through. Diffusion at bigger pore is very much related to Knudsen flow. Abedini (2012) implied that the selectivity poses by Knudsen is very low.

Again, here, the high temperature applied may also break the force that holds the adsorbed molecules on the pore wall surface. As stated earlier, the diameter of CO_2 molecule is relatively smaller than CH_4. The sudden drop for separation factor for 0.2 nm is supported by result in Figure 5.4 where CH_4 permeability starts to increase.

Not only that, Safari (2009) said that the cost is proportion to its operating temperature which ultimately makes higher temperature less attractive. As a mixture, the CO_2 molecules will be trapped in CH_4 molecules' voids. At this point, CO_2, being a strongly diffusing gas will prevent CH_4 molecules from crossing the membrane, thus, raising the selectivity of the process.

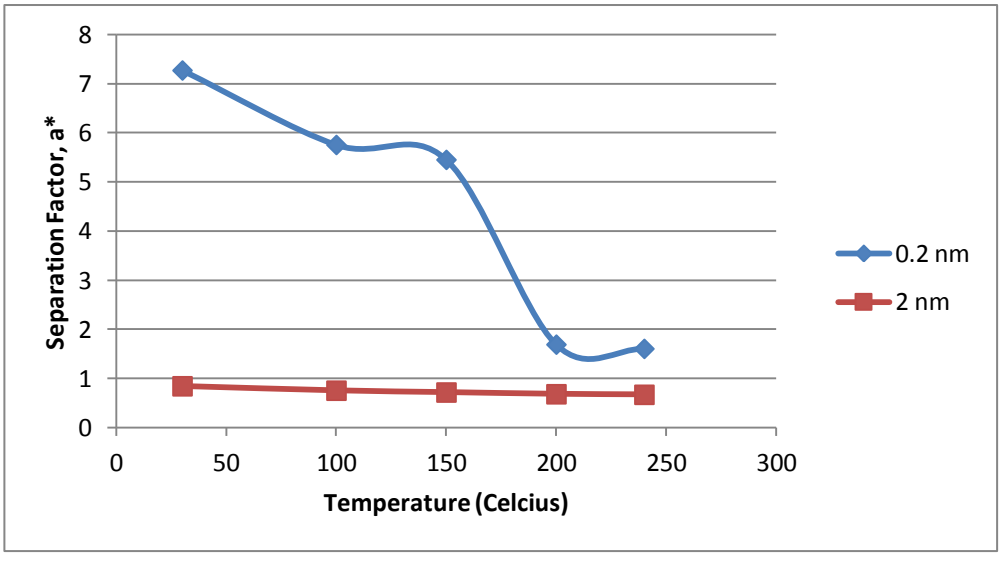

Figure 5.6: Comparison of CO_2 and CH_4 Separation Factor at Various Operating Temperature with Different Pore Size (P = 60 atm).

5.5 The Effect of Stage Cut and Feed CO_2 Composition on Separation Performance

Stage cut is defined as the ratio of permeate flow to feed flow. Higher stage cut means the flow of permeate (CO_2 removed side) is higher. It was briefly stated in Chapter 1 that one of the problems in membrane gas separation is the loss of CH_4 in the permeate stream. Comparing Figure 5.7 and 5.9, with higher stage cut, we can see the opposite behavior displayed where CO_2 removed is decreasing while CH_4 loss in the permeate side is increasing.

It is also seen that in Figure 5.7, as the feed CO_2 increases, the CO_2 removed is higher as the molecules gather more momentum due to collision with same species at the pore. The feed CO_2 concentration is kept below 70% as affirmed by Cakal (2012) that CH_4 permeation detected in the gas chromatograph is very limited in CO_2 rich mixtures. This result is agreeable by Boributh (2009) where CO_2 absorption flux increases by 7.0% with increasing feed CO_2 composition due to higher driving force applied compared to lower concentration. Chenar (2005) had stated that based on his experimental study on CO_2/CH_4 separation using polyimide hollow fibre membrane, at any feed CO_2 concentration, CO_2 removed decreases as stage cut increases. The effect is believed to be caused by the increment of polarization effect at higher stage cut.

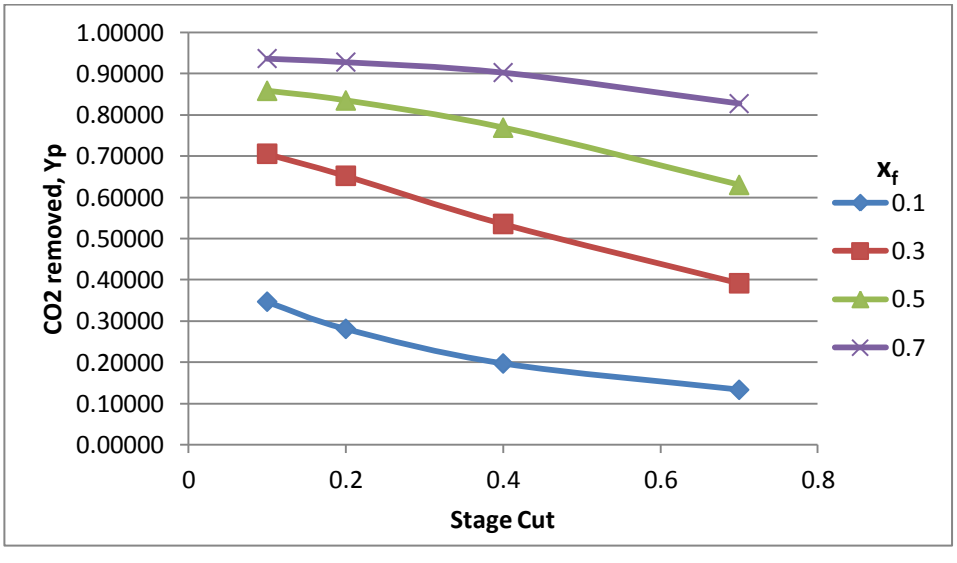

Figure 5.7: CO_2 Removed at Various Stage Cut with Different CO_2 Feed Composition, x_f (Pore Size = 0.2 nm, Pressure = 60 atm, Temperature = 303 K).

Not only that, typically, the pipeline quality requires only 2 % or less CO_2 retained (Safari, 2009). From Figure 5.8, the same increasing trends are observed for both retentate and permeate sides as the feed composition of CO_2 becomes higher. Also, at 10% feed CO_2 composition, the CO_2 retained would most likely to meet the pipeline specification.

The quality is greater when the system operates at higher stage cut. However, later in Figure 5.9, it is seen that higher stage cut will make the separation least attractive due to high losses of CH_4.

In a nutshell, a lower stage cut in cascaded setting will justify this separation as in cascade arrangement, the retained stream will be recycled back as feed for further treatment. The separation may require multiple stages in order to achieve the pipeline specification.

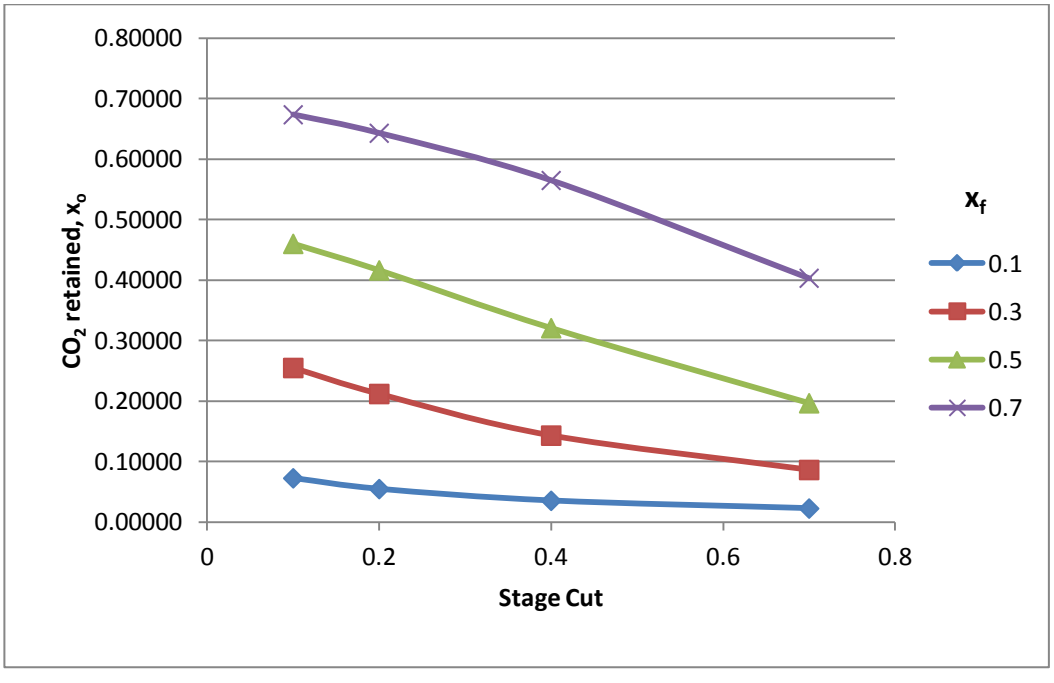

Figure 5.8: CO_2 Retained at Various Stage Cut with Different CO_2 Feed Composition, x_f (Pore Size = 0.2 nm, Pressure = 60 atm, Temperature = 303 K).

In addition to that, the CH_4 loss is also the minimum at lowest stage cut. The same relationship was also found in Norhayati's (2009) study on membrane gas dehydration where CH_4 loss is proportional to stage cut.

Even though at higher stage cut the quality of CH_4 stream is improved as the amount CO_2 retained is lower (more CO_2 removed), it will sacrifice higher CH_4 loss. Higher stage cut means lower feed flow which gives more contact time for the CH_4 to travel to the permeate side. The higher loss makes it less economically feasible.

Safari (2012) assured that acceptable CH_4 loss is around 2 to 10%. Based on Figure 5.9, the condition can only be adhered if the stage cut is 0.4 and below with 70% CO_2 feed concentration.

In lower feed CO_2 composition, the CH_4 loss is higher due to initial abundance presence of CH_4 molecules in the treated stream as compared to CO_2, which causes the probability for CH_4 losses to the permeate side higher. Satisfactory CH_4 recovery can be induced by recycling the permeate stream or using double stage configurations (Lau, 2010).

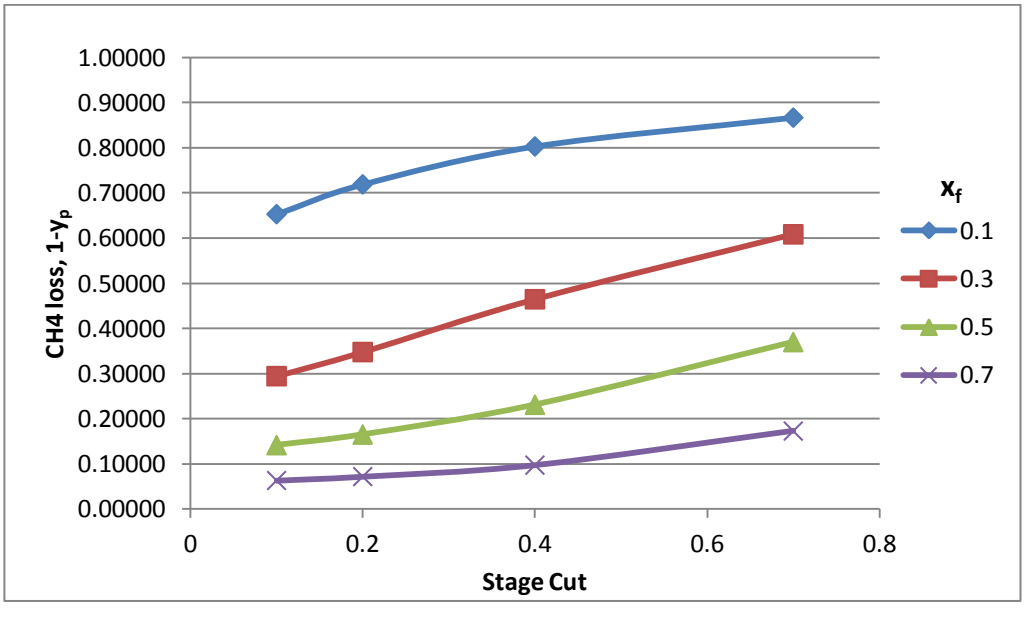

Figure 5.9: CH_4 Loss at Various Stage Cut with Different CO_2 Feed Composition, x_f

(Pore Size = 0.2 nm, Pressure = 60 atm, Temperature = 303 K).

CHAPTER 6

CONCLUSION AND RECOMMENDATIONS

This project is aimed to develop a mathematical model for CO_2-CH_4 separation using γ-alumina membrane and analyse parameters affecting permeability and separation behavior. Through the end, a simple yet specific mathematical model is successfully developed based on complete mixing model which is capable to simulate the permeability of the constituents in the chosen module as a function of various pore size, temperature and pressure. Not only that, separation factor is also determined with added process parameters such as stage cut and feed CO_2 composition.

The first part of the study dealt with the study of gas permeability as a function of pore size. As discussed earlier, at small pore, surface diffusion dominates while Knudsen diffusion dominates at big pore. The result shows that the smallest pore size, 0.2 nm will provide the most favourable permeation of CO_2 with better selectivity.

In the second part, the effect of operating pressure on gas permeability resulted that higher pressure will increase overall permeability. However, higher pressure is to be avoided due to increase in cost and risk. From the result, 60 atm is selected as the best operating pressure based on higher permeability provided at reasonably high pressure.

The third part is the effect of operating temperature on gas permeability. Holistically, the temperature increment causes the permeability to decrease as less adsorbed molecules on wall surface. Therefore, the optimum temperature is said to be at 303 K.

The result also shows that small pore size gives better selectivity as compared to big pore for the fourth part where the effect of temperature on separation factor study. This is thoroughly explained as the higher mean free path reduces the selectivity of the separation.

Lastly, the effect of stage cut and feed CO_2 composition on separation performance is analysed. Higher stage cut will give lower removal of CO_2, lower CO_2 retained and higher CH_4 loss. Meanwhile, the higher feed CO_2 will give more momentum for CO_2 removal and CO_2 retained. From result obtained, at lowest stage cut, 0.1 and 10% feed CO_2 composition, the CO_2 retained would most likely to meet the pipeline specification with lower hydrocarbon losses. In a nutshell, a lower stage cut in cascaded setting will justify this separation as in cascade arrangement, the

retained stream will be recycled back as feed for further treatment. The separation may require multiple stages in order to achieve the pipeline specification.

Among the possible recommendations for this project is relating to improving this study by incorporating additional elements to perfect the model prediction.

i. Future work can assimilate the counter current flow and cross flow model as opposed to complete mixing model as it is claimed to be more cost-effective in the industry.
ii. As explained earlier in Chapter 2, hydrocarbon losses occur and can be prevented by using a multi-stage process. For that reason, future research can be done by using multiple stages. Not only that, cascade arrangement study would benefit this separation too.
iii. The model used is assumed to operate in an isothermal manner. Nevertheless, cooling and heating activities may be taken into considerations as it may cause expansion in the membrane module. This includes the pore expansion as the temperature rises.
iv. Essential tuning can be done towards the model to improve the model reliability. As examples, there are several extended empirical models such as Dusty Gas Model which takes into account overall transport contributions. Meanwhile, P-D Model is closely reflecting the actual characteristic of a real membrane.
v. It is also strongly suggested to taken into account the effect of capillary condensation transport mechanism especially at low temperature and high pressure.

REFERENCES

1. **A.J. Burggraaf, L. Cot (1996),** *'Fundamentals of Inorganic Membrane Science and Technology'.*
2. **Angelo Basile, Fausto Gallucci (2011),** *'Membranes for Membrane Reactor: Preparation, Optimization & Selection',* Wiley, pg 7-8.
3. **Binay K. Dutta (2007),** *'Principles of Mass Transfer and Separation Process',* Eastern Economy Edition, Chapter 14 Membrane Separation, pg 728.
4. **Bird, R.B. (1960),** 'Transport Phenomena', Wiley.
5. **C.J. Geankoplis (2003),** *'Transport Processes and Separation Process Principles',* Prentice Hall.
6. **Endre Nagy (2011),** *'Basic Equations of the Mass Transport Through a Membrane Layer',* Elsevier, pg 192.
7. **H. Mukhtar (2010),** *'Comparison of Predictive Models for Relative Permeability of CO_2 in Matrimid-Carbon Molecular Sieve Mixed Matrix Membrane',* Journal of Applied Science, pg 1204-1211.
8. **Himeno (2007),** *'Synthesis and Permeation Properties of a DDR-Type Zeolite Membrane for Separation of CO_2/CH_4 Gaseous Mixtures',* Ind. Eng. Chem. Res. 46,pg 6989-6997.
9. **Kang Li (2007),** *'Ceramic Membranes for Separation and Reaction',* Wiley, pg 123-125.
10. **Kazama (2004),** 'CO_2 Separation with Molecular Gate Membrane', Research Institute of Innovative Technology for the Earth Chemical Research Group (RITE)
11. **Lau Kok Keong, Fazian Ahmad, Azmi Mohd. Shariff (2010),** *'Modeling and Parametric Study for CO_2/CH_4 Separation using Membrane Processes',* World Academy of Science, Engineering and Technology, Vol. 48.
12. **M. Pourafshar Chenar, M. Soltaneih, T. Matsuura, A. Tabe-Mohammadi (2005),** 'The *CO_2/CH_4 Separation by Commercially Available PPO and Cardo-type Polyimide Hollow Fiber Membranes',* Industrial Membrane Research Institute.
13. **M. Sim (2005),** *'MATLAB',* Department of Decision Sciences, NUS Business School.
14. **Maria L. Carreon, Shiguang Li, Moises A. Carreon (2012),** *'AIPO-18 Membranes for CO_2-CH_4 Separation',* The Royal Society of Chemistry.

15. **Mohammadhosein Safari (2008),** *'Optimization of Membrane-based CO2 Removal from Natural Gas using Simple Models Considering Both Pressure and Temperature Effects',* International Journal of Greenhouse Gas Control 3.
16. **Nadine Schmeling (2010),** *'Functionalized Copolyimide Membranes for the Separation of Gaseous and Liquid Mixtures',* Beilstein Journal of Organic Chemistry.
17. **Norhayati Mellon, Azmi M. Shariff, Lau Kok Keong (2009),** *'A Theoritical Analysis of Natural Gas Dehydration Using Membrane Processes',* Department of Chemical Engineering, Universiti Teknologi PETRONAS (UTP).
18. **Okada M, Nakagawa H (1989),** *'Purification and Characterization of Membrane-bound Inositolpolyphosphate 5-phosphatase'*, Journal of Biochem.
19. **Reza Abedini, Amir Nezhamoghadam (2010),** *'Application of Membrane in Gas Separation Processes: Its Suitability and Mechanisms',* Petroleum and Coal, pg 69-80.
20. **S. S. Madaeni, G Zahedi (2010),** *'A Mathematical Method to Study CO_2-CH_4 Separation in a Hollow Fibre Module',* Indian Journal of Chemical Technology.
21. **Simon Judd, Bruce Jefferson (2003),** *'Membranes for Industrial Wastewater Recovery and Re-use',* Elvesier, pg 7.
22. **Somnuk Boributh, Suttichai Assabumrungrat, Navadol Laosiripojana, Ratana Jiraratananon (2011),** *'A Modeling Study on the Effects of Membrane Characteristics and Operating Parameters on Physical Absorption of CO_2 by Hollow Fiber Membrane Contactor',* Journal of Membrane Science, pg 21-33.
23. **Spillman, Sherwin (2011),** *'Gas Permeation for Separation Process'.*
24. **Stern, S.A. (1969),** *'Analysis of Membrane Separation Parameter',* Separation Science, pg 129-159.
25. **Synkera (2010),** *'Nanoporous Ceramic Membranes Technology Profile'.*
26. **Ulgen Cakal, Levent Yilmaz, Halil Kalipcilar (2012),** *'Effect of Feed Gas Composition on the Separation of CO_2/CH_4 Mixtures by PES-SAPO 34-HMA Miced Matrix Membranes',* Journal of Membrane Science, pg 45-51.
27. **Weller, S., W.A. Steiner. (1950),** *'Separation of Gases by Fractional Permeation through Membranes',* Journal of Applied Physics, Vol. 21, pg 180.
28. **Yu (2005),** *'Preparation of Meso-porous-γ-alumina Membrane',* The Ohio State University Group Inorganic Materials Science.

APPENDICES

Appendix A: Permeability vs. Pore Size Data Sheet & Result (at Pressure = 60 atm, Temperature = 303 K)

Pore Size	Permeability CO2	Permeability CH4
2E-10	4.16719E-11	5.73263E-12
1E-09	5.16864E-11	5.56372E-11
2E-09	1.04816E-10	1.29483E-10
3E-09	1.66014E-10	2.11544E-10
4E-09	2.33338E-10	3.01732E-10

Pore Size	Viscosity Diffusion		Viscosity Permeability		Knudsen Diffusion		Knudsen Permeability		Surface Diffusion		Surface Permeability	
	CO2	CH4	CO2	CH4	CO2	CH4	CO2	CH4	CO2	CH4	CO2	CH4
2E-10	2.21E+15	1.09E+15	1.348E-33	2.108E-33	8.91E-09	2.53E-09	1.71E-12	3.741E-13	7.67E-09	3.84E-09	3.996E-11	5.36E-12
1E-09	2.21E-05	1.09E-05	3.369E-12	5.27E-12	2.13E-07	3.4E-07	4.033E-11	4.93E-11	7.67E-09	3.84E-09	7.992E-12	1.07E-12
2E-09	2.21E-05	1.09E-05	1.348E-11	2.108E-11	4.67E-07	7.61E-07	8.734E-11	1.079E-10	7.67E-09	3.84E-09	3.996E-12	5.36E-13
3E-09	2.21E-05	1.09E-05	3.032E-11	4.743E-11	7.22E-07	1.18E-06	1.33E-10	1.638E-10	7.67E-09	3.84E-09	2.664E-12	3.57E-13
4E-09	2.21E-05	1.09E-05	5.39E-11	8.432E-11	9.76E-07	1.6E-06	1.774E-10	2.171E-10	7.67E-09	3.84E-09	1.998E-12	2.68E-13

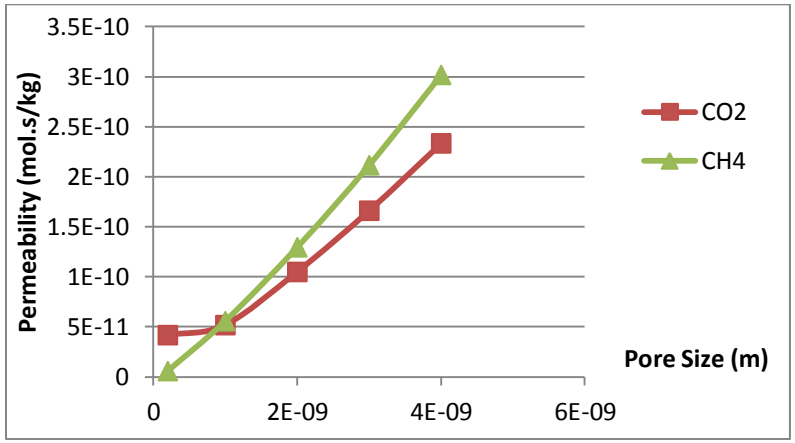

Appendix B: Permeability vs. Pressure Data Sheet & Result (at Pore Size = 0.2 nm, Temperature = 303 K)

Pressure	Z		f	
	CO2	CH4	CO2	CH4
40	0.7732	0.9897	0.0000618	2.15E-05
50	0.7643	0.9842	7.725E-05	2.69E-05
60	0.7515	0.9758	0.0000927	3.23E-05
70	0.7298	0.9658	0.0001	3.76E-05

Pressure	Permeability CO2	Permeability CH4
40	8.87772E-11	1.06882E-10
50	1.01878E-10	1.25097E-10
60	1.06814E-10	1.29753E-10
70	1.12743E-10	1.34709E-10

Pressure	Viscosity Diffusion		Viscosity Permeability		Knudsen Diffusion		Knudsen Permeability		Surface Diffusion		Surface Permeability	
	CO2	CH4	CO2	CH4	CO2	CH4	CO2	CH4	CO2	CH4	CO2	CH4
40	2.21E+15	1.088E+15	8.82E-32	1.3991E-31	4.67E-07	7.61E-07	8.489E-11	1.064E-10	7.67E-09	3.84E-09	3.88E-12	5.28E-13
50	2.21E-05	1.088E-05	1.11E-11	1.7484E-11	4.67E-07	7.61E-07	8.588E-11	1.069E-10	7.67E-09	3.84E-09	4.91E-12	6.65E-13
60	2.21E-05	1.088E-05	1.35E-11	2.1079E-11	4.67E-07	7.61E-07	8.734E-11	1.079E-10	7.67E-09	3.84E-09	5.99E-12	8.05E-13
70	2.21E-05	1.088E-05	1.61E-11	2.4777E-11	4.67E-07	7.61E-07	8.994E-11	1.09E-10	7.67E-09	3.84E-09	6.66E-12	9.47E-13

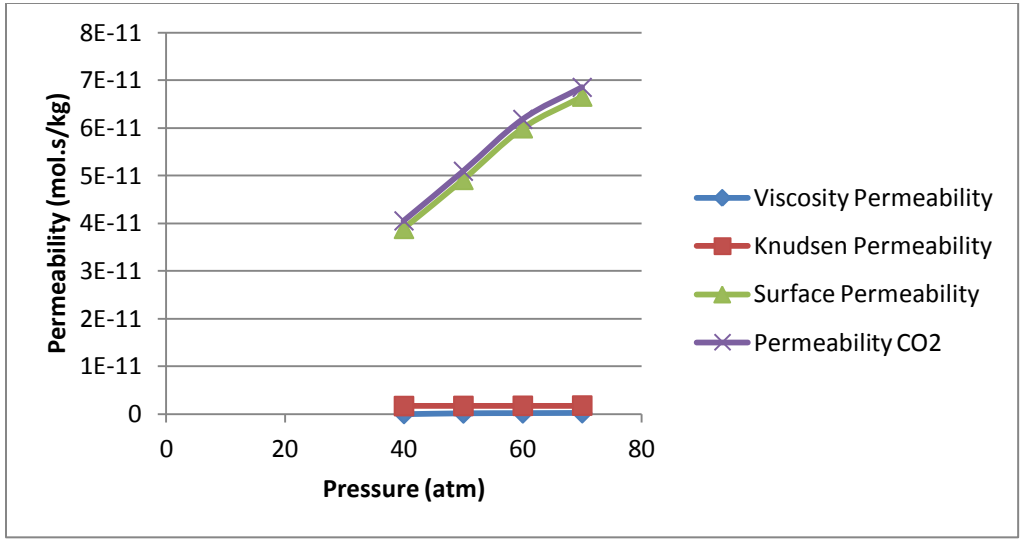
8E-11
7E-11
6E-11
5E-11
4E-11
3E-11
2E-11
1E-11
0
Permeability (mol.s/kg)
0
20
40
60
80
Pressure (atm)
Viscosity Permeability
Knudsen Permeability
Surface Permeability
Permeability CO2

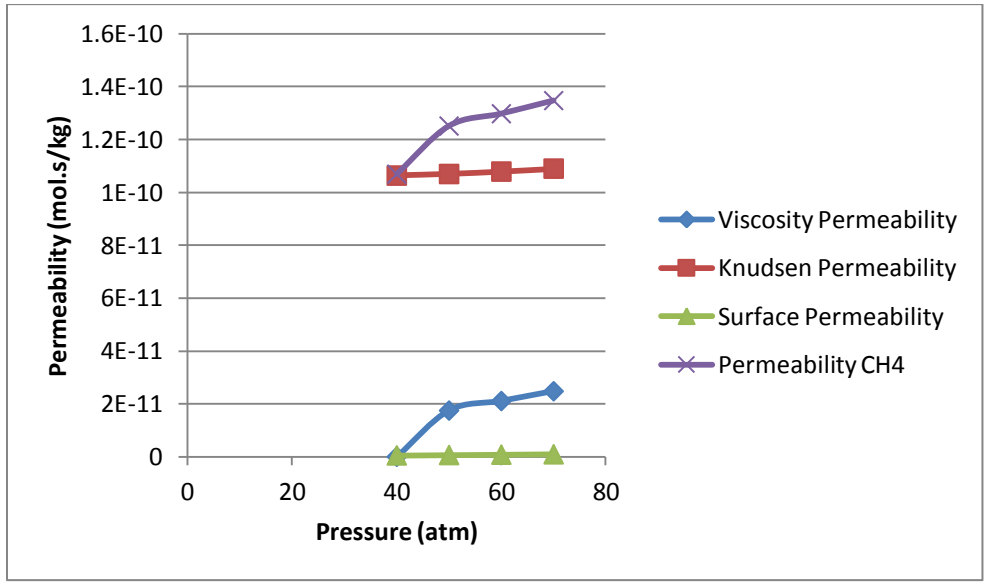
1.6E-10
1.4E-10
1.2E-10
1E-10
8E-11
6E-11
4E-11
2E-11
0
Permeability (mol.s/kg)
0
20
40
60
80
Pressure (atm)
Viscosity Permeability
Knudsen Permeability
Surface Permeability
Permeability CH4

Appendix C: Permeability vs. Temperature Data Sheet & Result (at Pore Size = 0.2 nm, Pressure = 60 atm)

Temperature	Z		f	
	CO2	CH4	CO2	CH4
30	0.7515	0.9758	0.0000618	0.0000215
100	0.8435	0.9806	0.0000348	0.0000121
150	0.8954	0.9876	0.0000286	0.00000994
200	0.9473	1.0031	0.0000248	0.00000863
240	0.9812	1.0205	0.0000227	0.00000863

Temperature	Permeability CO2	Permeability CH4
30	4.16719E-11	5.73263E-12
100	3.0242E-11	5.25623E-12
150	2.76301E-11	5.38249E-12
200	2.54786E-11	1.50766E-11
240	2.41528E-11	1.50615E-11

Temperature	Viscosity Diffusion		Viscosity Permeability		Knudsen Diffusion		Knudsen Permeability		Surface Diffusion		Surface Permeability	
	CO2	CH4	CO2	CH4	CO2	CH4	CO2	CH4	CO2	CH4	CO2	CH4
30	2.21E+15	1.09E+15	1.348E-33	2.108E-33	8.91E-09	2.5E-09	1.71E-12	3.741E-13	7.67E-09	4E-09	3.996E-11	5.36E-12
100	2.452E+15	1.21E+15	8.79E-34	1.536E-33	9.88E-09	2.8E-09	1.373E-12	3.356E-13	1.36E-08	8E-09	2.887E-11	4.92E-12
150	2.611E+15	1.29E+15	6.856E-34	1.263E-33	1.05E-08	3E-09	1.215E-12	3.129E-13	1.82E-08	1E-08	2.642E-11	5.07E-12
200	2.761E+15	1.36E+15	5.481E-34	1.051E-33	1.11E-08	3.2E-09	1.086E-12	2.913E-13	2.3E-08	1E-08	2.439E-11	1.48E-11
240	2.876E+15	1.42E+15	4.685E-34	9.149E-34	1.16E-08	3.3E-09	1.007E-12	2.749E-13	2.67E-08	2E-08	2.315E-11	1.48E-11

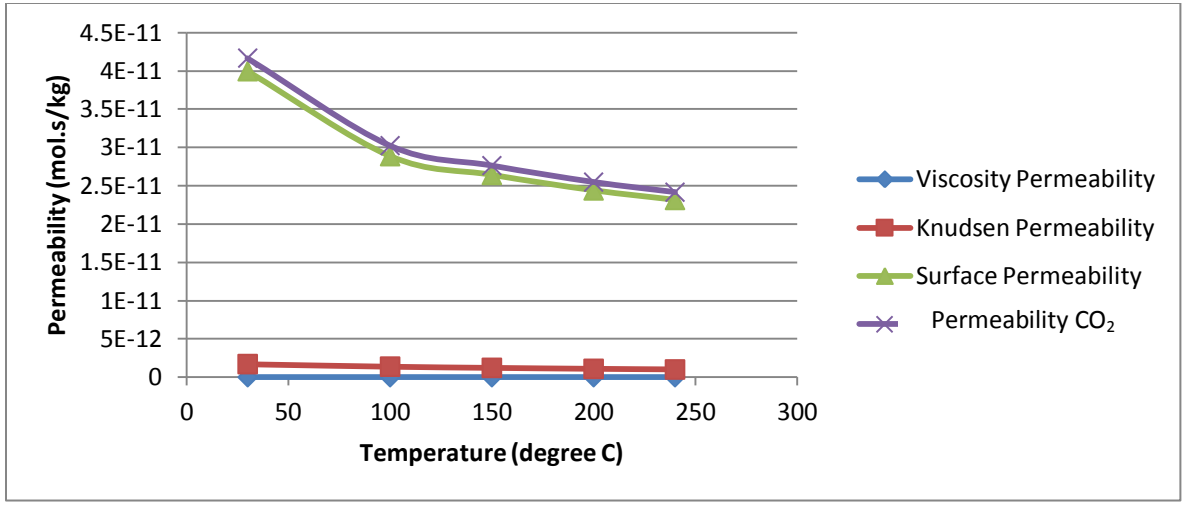
4.5E-11
4E-11
3.5E-11
3E-11
2.5E-11
2E-11
1.5E-11
1E-11
5E-12
0
Permeability (mol.s/kg)
0
50
100
150
200
250
300
Temperature (degree C)
Viscosity Permeability
Knudsen Permeability
Surface Permeability
Permeability CO_2

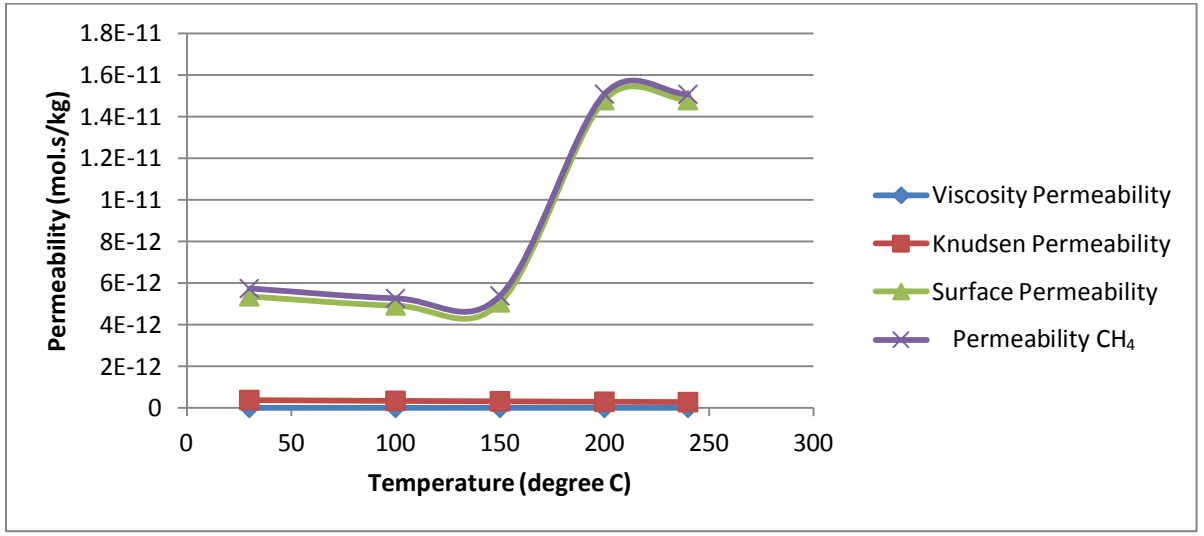
1.8E-11
1.6E-11
1.4E-11
1.2E-11
1E-11
8E-12
6E-12
4E-12
2E-12
0
Permeability (mol.s/kg)
0
50
100
150
200
250
300
Temperature (degree C)
Viscosity Permeability
Knudsen Permeability
Surface Permeability
Permeability CH_4

Appendix D: Permeability vs. Temperature Data Sheet & Result (at Pore Size = 2 nm, Pressure = 60 atm)

Temperature	Z		f	
	CO2	CH4	CO2	CH4
30	0.7515	0.9758	0.0000618	0.0000215
100	0.8435	0.9806	0.0000348	0.0000121
150	0.8954	0.9876	0.0000286	0.00000994
200	0.9473	1.0031	0.0000248	0.00000863
240	0.9812	1.0205	0.0000227	0.00000863

Temperature	Permeability CO2	Permeability CH4
30	9.13406E-11	1.08404E-10
100	7.28216E-11	9.67913E-11
150	6.43895E-11	9.00233E-11
200	5.75351E-11	8.45864E-11
240	5.33218E-11	7.97504E-11

Temperature	Viscosity Diffusion		Viscosity Permeability		Knudsen Diffusion		Knudsen Permeability		Surface Diffusion		Surface Permeability	
	CO2	CH4	CO2	CH4	CO2	CH4	CO2	CH4	CO2	CH4	CO2	CH4
30	2.21E+15	1.1E+15	1.3475E-31	2.11E-31	4.67E-07	7.6E-07	8.734E-11	1.08E-10	7.67E-09	4E-09	3.996E-12	5.36E-13
100	2.452E+15	1.2E+15	8.7898E-32	1.54E-31	5.182E-07	8.4E-07	6.993E-11	9.63E-11	1.36E-08	8E-09	2.887E-12	4.92E-13
150	2.6112E+15	1.3E+15	6.8565E-32	1.26E-31	5.518E-07	9E-07	6.175E-11	8.95E-11	1.82E-08	1E-08	2.642E-12	5.07E-13
200	2.7612E+15	1.4E+15	5.4809E-32	1.05E-31	5.835E-07	9.5E-07	5.51E-11	8.31E-11	2.3E-08	1E-08	2.439E-12	1.48E-12
240	2.8756E+15	1.4E+15	4.6848E-32	9.15E-32	6.077E-07	9.9E-07	5.101E-11	7.83E-11	2.67E-08	2E-08	2.315E-12	1.48E-12

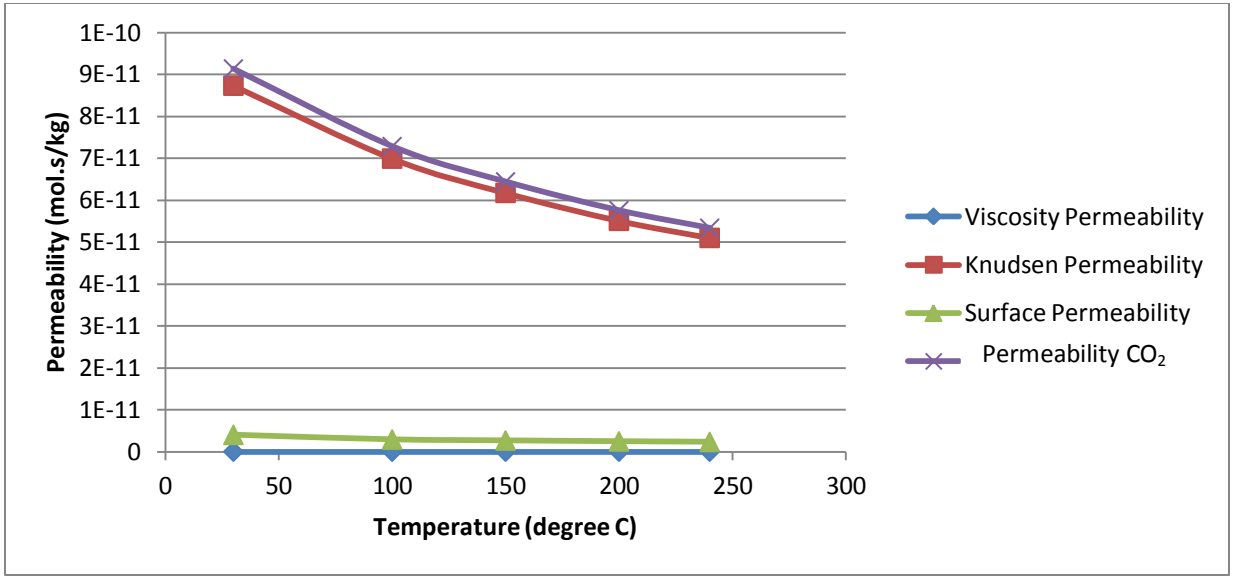
1E-10
9E-11
8E-11
7E-11
6E-11
5E-11
4E-11
3E-11
2E-11
1E-11
0
Permeability (mol.s/kg)
0
50
100
150
200
250
300
Temperature (degree C)
Viscosity Permeability
Knudsen Permeability
Surface Permeability
Permeability CO_2

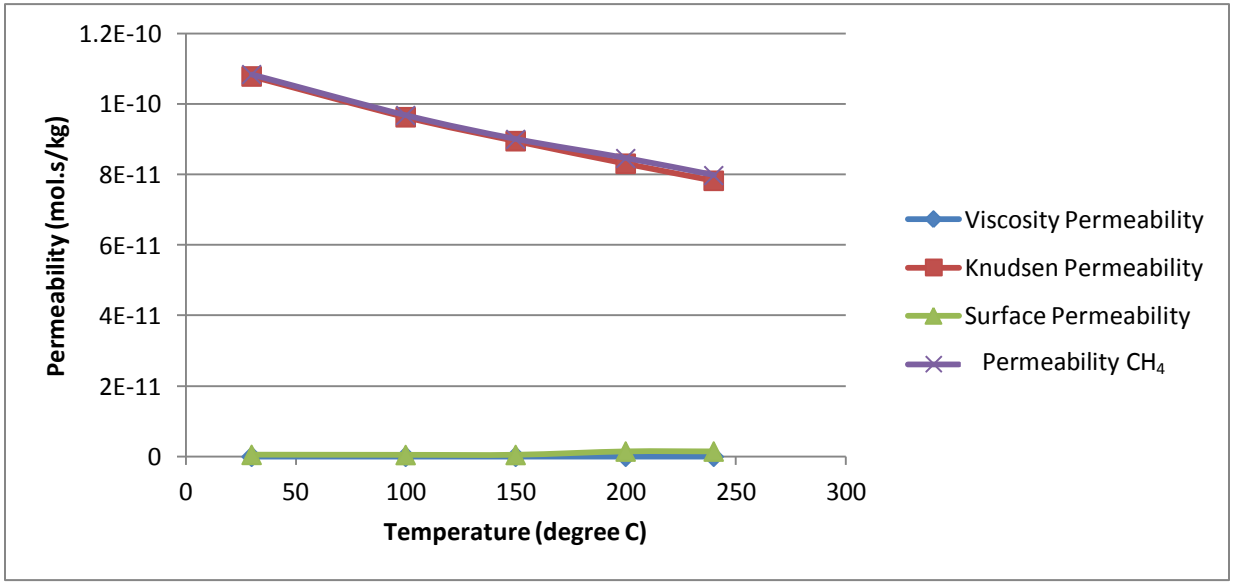
1.2E-10
1E-10
8E-11
6E-11
4E-11
2E-11
0
Permeability (mol.s/kg)
0
50
100
150
200
250
300
Temperature (degree C)
Viscosity Permeability
Knudsen Permeability
Surface Permeability
Permeability CH_4

Appendix E: Ideal Separation Factor, a* vs Temperature (at Pore Size = 0.2 nm & 2 nm, Pressure = 60 atm)

Pore Size (nm)	0.2 nm	2 nm	Temperature (degree C)
a*	7.269244	0.842592	30
	5.753549	0.752357	100
	5.449994	0.715254	150
	1.68994	0.680193	200
	1.603614	0.668609	240

Appendix F: Composition Balance around Membrane Using Complete Mixing Model (at Pore Size = 0.2 nm, Pressure = 60 atm, Temperature = 303 K)

Pressure ratio, pL/pH	a*	Stage Cut	Feed CO2, Xf	Yp guess	CO2 retain	CO2 remove	CH4 loss	Error (%)	Check total
					Xo calc	Yp calc			
0.017	7.3	0.2	0.1	0.28104	0.05474	0.28104	0.71896	0.00066	1.00000
			0.3	0.65216	0.21196	0.65216	0.34784	0.00149	1.00000
			0.5	0.83480	0.41630	0.83480	0.165203	-0.000343	1.00000
			0.7	0.92791	0.64302	0.92791	0.07209	-0.00013	1.00000
		0.7	0.1	0.13320	0.02253	0.13320	0.86680	0.00190	1.00000
			0.3	0.39158	0.08630	0.39158	0.60842	-0.00039	1.00000
			0.5	0.63001	0.19664	0.63001	0.36999	-0.00062	1.00000
			0.7	0.82716	0.40330	0.82716	0.17284	0.00042	1.00000
		0.1	0.1	0.34689	0.07257	0.34689	0.65311	0.00011	1.00000
			0.3	0.70557	0.25494	0.70557	0.29443	0.00037	1.00000
			0.5	0.85822	0.46020	0.85822	0.14178	0.00024	1.00000
			0.7	0.93657	0.67371	0.93657	0.06343	-0.00031	1.00000
		0.4	0.1	0.19703	0.03532	0.19703	0.80297	0.00163	1.00000
			0.3	0.53535	0.14310	0.53535	0.46465	0.00005	1.00000
			0.5	0.76885	0.32077	0.76885	0.23115	0.00001	1.00000
			0.7	0.90252	0.56498	0.90252	0.09748	0.00001	1.00000